Methods and guidelines for the choice of shell theories

Noname manuscript No.
(will be inserted by the editor)

Methods and guidelines for the choice of shell theories

Marco Petrolo · Erasmo Carrera

the date of receipt and acceptance should be inserted later

Abstract This paper provides an overview of the modeling approaches adopted over the years to develop shell theories for composite structures. Furthermore, it presents a method to assess any structural theory concerning the accuracy and computational efficiency and trigger informed decisions on the structural theory to use for a given problem. This method exploits the synergies between the Carrera Unified Formulation (CUF) and the Axiomatic/Asymptotic Method (AAM). Typical outcomes are the Best Theory Diagrams (BTD) or the estimation of accuracy of a theory as compared to quasi-3D solutions. The proposed framework can be useful to provide guidelines on the construction of structural theories and can serve as a trainer for the deep learning of neural networks.

Keywords Shell · FEM · Composites · Shear deformation · Transverse stretching

1 Introduction

Shell theories are two-dimensional (2D) mathematical models based on assumed variable distributions acting along the thickness direction. The use of shells leads to reduced computational costs if compared to 3D models. A common solution strategy for engineering problems is the finite element method (FEM). The computational cost of a shell finite element stems from the number of nodes on the reference surface and the nodal unknowns depending on the assumed distribution along the thickness.Shell elements in commercial codes

M. Petrolo
MUL^2 Group, Department of Mechanical and Aerospace Engineering, Politecnico di Torino, Italy. E-mail: marco.petrolo@polito.it

E. Carrera
MUL^2 Group, Department of Mechanical and Aerospace Engineering, Politecnico di Torino, Italy E-mail: erasmo.carrera@polito.it

rely on the classical theories of structures [1–6]. Focusing on the use of classical 2D elements, such as four, eight and nine node ones, i.e., those elements widely adopted in non-academic realms, the maximum number of degrees of freedom (DOF) is six, namely, three displacements and rotations. Such theories consider unstretchable normals, are not reliable to consider the transverse mechanical characteristics of the material and fail at meeting the boundary conditions on the external surfaces. The validity of such structural models depends upon the problem in hand and the physical characteristics of the structure [7, 8]. To determine the applicability of classical models, one should consider several parameters, such as the thickness ratio, gradients in the strain and stress fields, anisotropy, and inhomogeneity. The reliability of classical models is high as soon as the structure is thin, there are no local effects, and in-plane stress, and transverse displacements are of interest. On the other hand, caution is necessary whenever the focus is on edge-effects, local distortions, higher-order oscillations, cracks, and contacts as transverse stresses and normal stretch become primarily important. Other examples of critical problems are those with multifield interactions such as thermal problems in which the material characteristics can change significantly and in an anisotropic manner. In the case of composite structures, typical features undermining classical assumptions are the following:

1. Moderately thick or thick structures, i.e., $\frac{a}{h} < 50$, where a is the characteristic length of the structure and h is the thickness.
2. Materials with high transverse deformability, e.g., common orthotropic materials, in which $\frac{E_L}{E_T}$, $\frac{E_L}{E_z} > 5$, and $\frac{G}{E_L} < \frac{1}{10}$, where E and G are the Young and shear moduli, and L is the fiber direction of the fiber and T, z are perpendicular to L.
3. Transverse anisotropy due to, for instance, the presence of contiguous layers with different properties.

As it is well-known, such factors require the proper modeling of shear and normal transverse stresses, and variations of the displacement field at the interface between two layers with different mechanical properties, i.e., the zig-zag effect. Most of the features are not present in isotropic materials; hence, the classical models can handle such structures. Since the last mid-century, scientists have become increasingly aware of the necessity of refining the classical models to provide more reliable predictions concerning composites [9–20].
The development of a structural theory aims at reducing the starting 3D problem to less cumbersome 2D or 1D ones. In 2D, the approximation acts via a through-the-thickness integration, and, in 1D, via an integral over the cross-section. The integration makes the unknown field dependent on the in-plane coordinates in the 2D case and the axial coordinate in the 1D case. Over the years, many approaches have emerged, and a tentative classification is as follows:

1. The method of hypotheses or axiomatic approach in which the mechanical behavior of a structure is postulated and then translated into mathematical constraints acting on the unknown variables, e.g., displacements, stresses,

stress resultants. The classical models, known as the Classical Lamination Theory (CLT) and the First Order Deformation Theory (FSDT), are the most known examples [4–6].

2. The method of expansions defines the unknown fields via thickness or cross-section expansions. Typically, this method uses polynomials and leads to higher accuracy and computational costs as the number of expansion terms augments [21]. However, the addition of new terms can be detrimental as soon as other equally important ones are not present. Also, some terms can have very little influence and lead to a pointless increase in the computational cost [22, 23], and it is not always possible to prove the convergence to the exact solution.
3. The asymptotic method [24, 25] starts from the 3D equations, identifies one or more characteristic parameter, e.g., the thickness ratio, and builds 2D or 1D expansions of the governing equations via that parameter to retain the terms up to a given order. Such a method provides a direct estimation of the accuracy of the solution as compared to the 3D exact one, but it may be very cumbersome as soon as, for example, the expansion must consider many problem parameters at the same time.

The expansion method, in a way, is a generalization of the hypothesis one as the addition of terms to the expansion can remove the assumptions and widen the applicability of the theory.
This paper aims at providing guidelines on the choice of structural models in the 2D case and for the linear analysis of composite structures. The first part of the paper is a literature overview of the most significant contributions concerning the development of structural theories. Given the significant number of papers on this topic, the authors preferred to focus on those works in which the development of the shell theory or the analysis of the higher-order terms is the primary aim. A review of the solution methods is not a scope of this paper but given, the importance of the topic, a brief overview follows.
Many efforts focused on the development of exact, analytical or semi-analytical solutions to verify numerical approaches. Leissa and Reddy are among the main contributors with special attention paid to 3D solutions and shear deformation theories [14, 26–33] or directly provide 3D solutions [34–39]. Other significant contributions are in [40–46]. The extension of exact solutions to wider cases focused on general boundary conditions and laminations [47–53], shells with cutouts [54], conical shape geometries [55], stiffened and damaged structures [56], and non-homogeneous properties [57]. Other solution schemes make use of various approaches. An example is the Galerkin method for higher-order models [58, 59], with mixed models based on the Reissner mixed variational method (RMVT) [60], and for conical shapes [61]. Another common solution is the Ritz and Rayleigh-Ritz with contributions on local boundary conditions [62, 63], arbitrary boundary conditions and complex shapes [64–68], 3D-like models [69, 70], sandwich structures [71], and comparisons with experimental results [72]. Other approaches are the spectral method for arbitrary boundary conditions and shapes [73], domain decomposition method [74–76], and the

differential quadrature method [77]. FEM has a great variety of contributions starting from early works a few decades ago [78–80]. Then, research focused on the element type, i.e., four- [81–83], eight- [84, 85], and nine-node elements [86, 87], the order of the structural model [88–93], the inclusion of transverse stretching and continuity [94–96], the development of solid-shell elements [97–105], and the improvement of FE performances regarding membrane and shear locking [106, 107], mesh accuracy [108], and distortion [109].
The second part of this paper is a proof of concept concerning a methodology for the evaluation of the accuracy and computational efficiency of a structural theory. The second part aims to answer the following questions:

1. Given a structural problem, what is the computationally cheapest and most accurate structural theory to use?
2. Given a structural theory, how does it compare to quasi-3D solutions concerning computational costs and accuracy?
3. Given an expansion of unknown variables, what are the terms to retain?

The assessment method stems from the latest developments concerning the use of the axiomatic/asymptotic method (AAM) [22, 23] to evaluate the accuracy of any-order shell model. The AAM leads to two primary outcomes, the best Theory Diagram (BTD) [110] and the Relevance Factor (RF) [111]. The former is a 2D plot to localize a shell model via its nodal degrees of freedom and accuracy. The latter is a parameter providing the relevance of a generalized variable or a set of variables. The present paper shows, for the first time, results concerning the AAM for the free vibration analysis via shell finite elements. In the past, AAM results on structural dynamics focused on beam finite elements [112] and the static analysis of shell elements [111]. In all cases, the Carrera Unified Formulation (CUF) [113] is the theoretical framework providing the governing equations for all the structural models, independently of the order of the theory or the completeness of the expansions.
This paper is organized as follows: the review of existing theories is in Section 2, CUF for FE shell in 3, the AAM and BTD in 4 and 5, the numerical examples in Section 6, the perspectives on the use of neural networks in Section 7, and conclusions in Section 8.

2 Challenging features of composites and review of shell theories

The development of structural theories for composites moved from the already available models for metallic structures to incorporating mechanical features typical of commonly used layered structures.
The first material property to handle is the in-plane anisotropy, i.e., the properties of each layer can change significantly depending on directions. The anisotropy may coexist with high transverse shear and normal flexibility and couplings between axial and shear strains. As mentioned above, there may be one order of magnitude of difference between Young's moduli for different directions and two orders between Young's and shear moduli. Further couplings

can arise between in-plane and out-of-plane strains, e.g., in the case of non-symmetric stacking sequences.
The second material feature requiring proper structural modeling is the transverse anisotropy stemming from layer-wise discontinuous physical properties along the thickness leading to compatibility and equilibrium conditions challenging to model. The compatibility requires the discontinuity of the slopes of displacement components at the layer interfaces, i.e., the zig-zag shape of the displacement field. Such a zig-zag shape must coexist with the equilibrium conditions dictating the continuity of the transverse stresses at the interfaces, i.e., transverse shear and axial stresses must be interlaminar continuous. The literature refers to the sum of the two conditions as to the C_0^z requirement.
The modeling challenges concerning such critical features can grow further in many scenarios, among others, the analysis of residual stress from the curing process, the analysis of damaged structures, the presence of singularities such as free-edges, the use of tens of layers, and the use of sandwich structures with soft cores.
This section provides an overview of the main approaches proposed in the last decades to use shell models for composites. After introducing first-order models, the aim is to present the main features of more sophisticated theories. One of the tools adopted to evaluate a theory is the Koiter recommendation [11] stating that refinements of structural theories have to consider the effects of transverse shear and normal stresses at the same time as these two effects have comparable importance. As analytically proved by Vetyukov [114], the curvature of the structural component leads to shear and normal stress distributions of the same asymptotic order of smallness.
The introduction of shell theories will follow a common notation in which the displacement field $\mathbf{u}$ has three components - u_α, u_β, and u_z - according to the reference system is in Fig. 1.

2.1 Classical Lamination and First-Order Shear Deformation Theories, CLT and FSDT

CLT stems from the use of the Kirchhoff theory [1–4]. An alternative way to indicate this theory is as Love First Approximation Theory (LFAT) [115] grouping all those models neglecting transverse shear stress and normal stretching. The displacement field of CLT has 3 unknowns, namely, the displacements u_{α_1}, u_{β_1}, and u_{z_1},

$$\begin{aligned} u_\alpha &= u_{\alpha_1} - z\, u_{z_1,\alpha} \\ u_\beta &= u_{\beta_1} - z\, u_{z_1,\beta} \\ u_z &= u_{z_1} \end{aligned} \tag{1}$$

The derivatives of the transverse displacement have the physical meaning of rotations of the normals, i.e., $\phi_\alpha = -u_{z_1,\alpha}$ and $\phi_\beta = -u_{z_1,\beta}$. The first hypothesis removed concerns the transverse shear and, considering a constant shear

distribution along the thickness, the displacement field becomes

$$\begin{aligned} u_\alpha &= u_{\alpha_1} + z\, u_{\alpha_2} \\ u_\beta &= u_{\beta_1} + z\, u_{\beta_2} \\ u_z &= u_{z_1} \end{aligned} \tag{2}$$

This is the FSDT model falling in the Love Second Approximation Theory (LSAT) class. The FSDT has 5 unknowns and the additional two terms are rotations of the normals corrected by shear, i.e., $u_{\alpha_2} = \phi_\alpha = \epsilon_{\alpha z}$-$u_{z_1,\alpha}$. FSDT is commonly available in commercial codes due to its computational efficiency and reliability in many engineering applications. Over the years, modified versions of FSDT allowed to fulfill the homogeneous top/bottom boundary conditions [116]. Other significant contributions based on FSDT are reported in [26, 30, 43, 61, 117, 118].

2.2 Higher-order theories

The enrichment of the displacement field is one of the most successful approaches to refine a structural theory. As pointed out by Washizu [21], a 2D or 1D model based on an infinite expansion would guarantee the exact 3D solution. Infinite expansions are not feasible. Therefore, truncated ones are of practical interest. The selection of the terms to retrieve is not a trivial task, and one of the aims of this paper is to propose an approach to handle this task.
Using a third-order polynomial expansion, referred to as N=3, the displacement field is as follows:

$$\begin{aligned} u_\alpha &= u_{\alpha_1} + z\, u_{\alpha_2} + z^2\, u_{\alpha_3} + z^3\, u_{\alpha_4} \\ u_\beta &= u_{\beta_1} + z\, u_{\beta_2} + z^2\, u_{\beta_3} + z^3\, u_{\beta_4} \\ u_z &= u_{z_1} + z\, u_{z_2} + z^2\, u_{z_3} + z^3\, u_{z_4} \end{aligned} \tag{3}$$

All three displacement components have complete expansions and, overall, twelve unknowns. In FE, such a model leads to twelve DOF per node. N=3 improves FSDT by allowing parabolic distributions of transverse shear and thickness stretching. Many third-order models do not consider the thickness stretching, e.g.,

$$\begin{aligned} u_\alpha &= u_{\alpha_1} + z\, u_{\alpha_2} + z^2\, u_{\alpha_3} + z^3\, u_{\alpha_4} \\ u_\beta &= u_{\beta_1} + z\, u_{\beta_2} + z^2\, u_{\beta_3} + z^3\, u_{\beta_4} \\ u_z &= u_{z_1} \end{aligned} \tag{4}$$

Other examples of higher-order expansions enhance FSDT via parabolic transverse displacements, such as the following seven DOF model:

$$\begin{aligned} u_\alpha &= u_{\alpha_1} + z\, u_{\alpha_2} \\ u_\beta &= u_{\beta_1} + z\, u_{\beta_2} \\ u_z &= u_{z_1} + z\, u_{z_2} + z^2\, u_{z_3} \end{aligned} \tag{5}$$

The inclusion of the parabolic distribution is significant in many cases, such as non-symmetric laminations.

Based on this approach, many important papers are in the literature. A tentative classification is on the presence or absence of thickness stretching. Works proposing models without stretching are in [28, 45, 89, 91, 119–121]. On the other hand, higher-order models fulfilling the Koiter recommendations are in [40–42, 90, 122–131].
Other classes of higher-order theories consider non-polynomial terms to build expansions [132–136]. Sinusoidal and exponential terms are typical choices, e.g.,

$$\begin{aligned} u_\alpha &= u_{\alpha_1} + z\, u_{\alpha_2} + sin(z\pi/h)\, u_{\alpha_3} + e^{z/h}\, u_{\alpha_4} \\ u_\beta &= u_{\beta_1} + z\, u_{\beta_2} + sin(z\pi/h)\, u_{\beta_3} + e^{z/h}\, u_{\beta_4} \\ u_z &= u_{z_1} + z\, u_{z_2} + sin(z\pi/h)\, u_{z_3} + e^{z/h}\, u_{z_4} \end{aligned} \tag{6}$$

Non-polynomial terms enrich the displacement field allowing the detection of more complex through-the-thickness distributions.

2.3 Zig-zag expansions

The necessity of zig-zag models stems from the difficulties in fulfilling the C_z^0 requirements via higher-order expansions. The increase of the order, in fact, is not enough to meet C_z^0 and transverse stresses distributions may be wrong if calculated via the Hooke law. Zig-zag theories can provide C_z^0; in other words, they can lead to structural theories fulfilling the compatibility and equilibrium conditions at the layer interface.
Zig-zag approaches trace back to the first half of the twentieth-century [9]. A complete review of zig-zag is beyond the scope of this paper but is available in [137] providing the main features of the three fundamental zig-zag approaches, namely, the Lekhnitskii [9], Ambartsumian [138], and Reissner-Murakami [139]. Other significant works focused on shells are [140–149]. An example of a zig-zag model enhancing FSDT is the following:

$$\begin{aligned} u_\alpha &= u_{\alpha_1} + z\, u_{\alpha_2} + (-1)^k\, \tfrac{2z_k}{h_k}\, u_{\alpha Z} \\ u_\beta &= u_{\beta_1} + z\, u_{\beta_2} + (-1)^k\, \tfrac{2z_k}{h_k}\, u_{\beta Z} \\ u_z &= u_{z_1} \end{aligned} \tag{7}$$

Where $u_{\alpha Z}$ and $u_{\beta Z}$ are two additional variables, referred to as Murakami's zig-zag functions, and the amount of DOF is still independent of the number of layers. Similarly, the zig-zag terms can enhance higher-order theories, e.g., the N=3 one,

$$\begin{aligned} u_\alpha &= u_{\alpha_1} + z\, u_{\alpha_2} + z^2\, u_{\alpha_3} + z^3\, u_{\alpha_4} + (-1)^k\, \tfrac{2z_k}{h_k}\, u_{\alpha Z} \\ u_\beta &= u_{\beta_1} + z\, u_{\beta_2} + z^2\, u_{\beta_3} + z^3\, u_{\beta_4} + (-1)^k\, \tfrac{2z_k}{h_k}\, u_{\beta Z} \\ u_z &= u_{z_1} + z\, u_{z_2} + z^2\, u_{z_3} + z^3\, u_{z_4} + (-1)^k\, \tfrac{2z_k}{h_k}\, u_{z Z} \end{aligned} \tag{8}$$

2.4 Layer-wise approach

The layer-wise approach introduces the dependency of the unknown variables on the number of layers. Such an approach leads to higher computational costs, but its adoption is necessary in many cases, e.g., the precise detection of stress in each layer, high-stress gradients along the thickness, free-edge and local effects. The use of a layer-wise approach leads to zig-zag distributions with the additional benefit of having independent layers. A layer-wise displacement field is the following:

$$\begin{array}{l} u_\alpha^k = L_1\, u_{\alpha_1}^k + L_2\, u_{\alpha_2}^k + \sum_{i=3}^{N} L_i u_{\alpha_i}^k \\ u_\beta^k = L_1\, u_{\beta_1}^k + L_2\, u_{\beta_2}^k + \sum_{i=3}^{N} L_i u_{\beta_i}^k \\ u_z^k = L_1\, u_{z_1}^k + L_2\, u_{z_2}^k + \sum_{i=3}^{N} L_i u_{z_i}^k \end{array} \tag{9}$$

L-functions are usually Lagrange or Legendre polynomials. To facilitate the application of compatibility conditions at the interfaces, '1' and '2' variables should have the physical meaning of displacements at the top and bottom of the interface, respectively. The other additional terms serve as higher-order ones to enrich the kinematics of each layer. Usually, the use of third- or fourth-order terms guarantees quasi-3D accuracy. Significant contributions on shell theories can be found in [150–161].

2.5 Reissner Mixed Variational Theorem, RMVT

In mixed formulations, displacements and stresses are primary variables [21]. The RMVT has emerged as one of the most powerful tools for composites and has as primary variables the displacements and the transverse stresses [162–164]. The use of RMVT is independent of the type of expansion adopted. In other words, Taylor expansions, zig-zag, layer-wise approaches and combination thereof remain available. For instance, a layer-wise model can have the following distributions of displacements and transverse stresses:

$$\begin{array}{l} u_\alpha^k = L_1\, u_{\alpha_1}^k + L_2\, u_{\alpha_2}^k + \sum_{i=3}^{N} L_i u_{\alpha_i}^k \\ u_\beta^k = L_1\, u_{\beta_1}^k + L_2\, u_{\beta_2}^k + \sum_{i=3}^{N} L_i u_{\beta_i}^k \\ u_z^k = L_1\, u_{z_1}^k + L_2\, u_{z_2}^k + \sum_{i=3}^{N} L_i u_{z_i}^k \\ \sigma_{\alpha z}^k = L_1\, \sigma_{\alpha z_1}^k + L_2\, \sigma_{\alpha z_2}^k + \sum_{i=3}^{N} L_i \sigma_{\alpha z_i}^k \\ \sigma_{\beta z}^k = L_1\, \sigma_{\beta z_1}^k + L_2\, \sigma_{\beta z_2}^k + \sum_{i=3}^{N} L_i \sigma_{\beta z_i}^k \\ \sigma_{zz}^k = L_1\, \sigma_{z z_1}^k + L_2\, \sigma_{z z_2}^k + \sum_{i=3}^{N} L_i \sigma_{z z_i}^k \end{array} \tag{10}$$

Carrera expanded these concepts and presented a generalized approach to building such models in a unified manner [165]. RMVT is convenient for multilayered structures. Interlaminar continuity of transverse stresses and zig-zag displacements are easily implementable, and post-processing for transverse stresses is not necessary. The extension of RMVT to a weak form of the Hooke law allows for the reduction in the computational costs with no accuracy penalties. Numerical examples proved that the use of an RMVT third-order zig-zag,

equivalent single-layer model can provide 3D-like accuracy in most cases except for severe local effects in which the layer-wise version is more preferable [113].

2.6 Asymptotic approaches

The construction of structural theories via the asymptotic method proceeds by defining a characteristic parameter of the structure and problem [24, 25]. Often, such a parameter is the ratio between the thickness and the in-plane dimension, i.e., $\epsilon = \mathrm{h/L}$. Then, ϵ leads to the following displacement field:

$$\boldsymbol{u} = \boldsymbol{u}_1 + \epsilon\, \boldsymbol{u}_2 + \epsilon^2\, \boldsymbol{u}_3 +, ..., +\epsilon^n\, \boldsymbol{u}_{n+1} + O(\epsilon^{n+1}) \tag{11}$$

The strain energy expression makes use of the previous expansion to isolate same-order terms. As the desired order is set, the expansion is truncated, and the problem solution proceeds via the minimization of the strain energy. The main advantage of this approach is the possibility to control the accuracy of the solution against the 3D one. Significant contributions for shells are reported in [166–178]. Moreover, recently, Vetyukov at al. [179] proposed a hybrid asymptotic/direct approach and demonstrated the asymptotic nature of the structural theory for elastic and piezoelectric shells, including the convergence to exact solutions even in the presence of essential heterogeneity and anisotropy for thin structures.

2.7 Proper generalized decomposition

One of the most recent techniques to build shell theories is the Proper Generalized Decomposition (PGD) [180–183]. The displacement field has two contributions, one from 2D FE and the other from thickness functions, as follows:

$$\begin{array}{l} u_\alpha = \sum_{i=1}^{N} P_\alpha^i(\alpha,\beta)\, T_\alpha^i(z) \\ u_\beta = \sum_{i=1}^{N} P_\beta^i(\alpha,\beta)\, T_\beta^i(z) \\ u_z = \sum_{i=1}^{N} P_z^i(\alpha,\beta)\, T_z^i(z) \end{array} \tag{12}$$

The strength of this method relies on the nonlinear iterative procedure allowing for the determination of the 2D and 1D functions. In other words, the choice of the displacement field and the solution of the problem merge.

3 Carrera unified formulation, CUF

CUF emerged as a generalized approach to generate any structural theory. Early works on shells, in which the CUF formalism was not present or not systematic, focused on the analysis of shear effects and transverse normal stress on composite shell buckling and vibrations [184, 185], use of RMVT for

structural dynamics [186] and statics [187–190]. The systematic use, analysis and list of guidelines and recommendations for RMVT and zig-zag are in [165] and [137, 191], respectively. The seminal works on the CUF formalism including a comprehensive numerical campaign date back to early 2000's [8, 113]. Following a work on exact solutions [192], the last decade focused on the finite element formulation [193–196]. The latest development of CUF introduced the concept of node-dependent kinematics (NDK) in which each node of an FE model can assume a different shell theory [197, 198].
The CUF displacement field for a 2D model is

$$\mathbf{u}(x,y,z) = F_\tau(z)\mathbf{u}_\tau(x,y) \qquad \tau = 1,\dots,M \tag{13}$$

The Einstein notation acts on τ. F_τ are the thickness expansion functions. $\mathbf{u}_\tau$ is the vector of the generalized unknown displacements. M is the number of expansion terms. In the case of polynomial, Taylor-like expansions, a fourth-order model, referred to as N=4, has the following displacement field:

$$\begin{aligned} u_\alpha &= u_{\alpha_1} + z\,u_{\alpha_2} + z^2\,u_{\alpha_3} + z^3\,u_{\alpha_4} + z^4\,u_{\alpha_5} \\ u_\beta &= u_{\beta_1} + z\,u_{\beta_2} + z^2\,u_{\beta_3} + z^3\,u_{\beta_4} + z^4\,u_{\beta_5} \\ u_z &= u_{z_1} + z\,u_{z_2} + z^2\,u_{z_3} + z^3\,u_{z_4} + z^4\,u_{z_5} \end{aligned} \tag{14}$$

N=4 has fifteen nodal DOF. The order and type of expansion is a free parameter. Thus, the structure of the theory is an input of the analysis. The metric coefficients H^k_α, H^k_β and H^k_z of the k^{th} layer are

$$H^k_\alpha = A^k(1+z_k/R^k_\alpha), \quad H^k_\beta = B^k(1+z_k/R^k_\beta), \quad H^k_z = 1 \tag{15}$$

R^k_α and R^k_β are the principal radii of the middle surface of the k^{th} layer, A^k and B^k the coefficients of the first fundamental form of Ω_k, see Fig. 1. This paper focuses only on shells with constant radii of curvature with $\mathrm{A}^k = \mathrm{B}^k = 1$. The geometrical relations are

$$\begin{aligned} \boldsymbol{\epsilon}^k_p &= \left\{\epsilon^k_{\alpha\alpha}, \epsilon^k_{\beta\beta}, \epsilon^k_{\alpha\beta}\right\}^T = (\boldsymbol{D}^k_p + \boldsymbol{A}^k_p)\boldsymbol{u}^k \\ \boldsymbol{\epsilon}^k_n &= \left\{\epsilon^k_{\alpha z}, \epsilon^k_{\beta z}, \epsilon^k_{zz}\right\}^T = (\boldsymbol{D}^k_{n\Omega} + \boldsymbol{D}^k_{nz} - \boldsymbol{A}^k_n)\boldsymbol{u}^k \end{aligned} \tag{16}$$

where

$$\boldsymbol{D}^k_p = \begin{bmatrix} \frac{\partial_\alpha}{H^k_\alpha} & 0 & 0 \\ 0 & \frac{\partial_\beta}{H^k_\beta} & 0 \\ \frac{\partial_\beta}{H^k_\beta} & \frac{\partial_\alpha}{H^k_\alpha} & 0 \end{bmatrix} \qquad \boldsymbol{D}^k_{n\Omega} = \begin{bmatrix} 0 & 0 & \frac{\partial_\alpha}{H^k_\alpha} \\ 0 & 0 & \frac{\partial_\beta}{H^k_\beta} \\ 0 & 0 & 0 \end{bmatrix} \qquad \boldsymbol{D}^k_{nz} = \begin{bmatrix} \partial_z & 0 & 0 \\ 0 & \partial_z & 0 \\ 0 & 0 & \partial_z \end{bmatrix} \tag{17}$$

$$\boldsymbol{A}^k_p = \begin{bmatrix} 0 & 0 & \frac{1}{H^k_\alpha R^k_\alpha} \\ 0 & 0 & \frac{1}{H^k_\beta R^k_\beta} \\ 0 & 0 & 0 \end{bmatrix} \quad \boldsymbol{A}^k_n = \begin{bmatrix} \frac{1}{H^k_\alpha R^k_\alpha} & 0 & 0 \\ 0 & \frac{1}{H^k_\beta R^k_\beta} & 0 \\ 0 & 0 & 0 \end{bmatrix} \tag{18}$$

The stress-strain relations are

$$\begin{aligned}\boldsymbol{\sigma}_p^k &= \left\{\sigma_{\alpha\alpha}^k, \sigma_{\beta\beta}^k, \sigma_{\alpha\beta}^k\right\}^T = \boldsymbol{C}_{pp}^k\boldsymbol{\epsilon}_p^k + \boldsymbol{C}_{pn}^k\boldsymbol{\epsilon}_n^k \\ \boldsymbol{\sigma}_n^k &= \left\{\sigma_{\alpha z}^k, \sigma_{\beta z}^k, \sigma_{zz}^k\right\}^T = \boldsymbol{C}_{np}^k\boldsymbol{\epsilon}_p^k + \boldsymbol{C}_{nn}^k\boldsymbol{\epsilon}_n^k\end{aligned} \tag{19}$$

where

$$\begin{aligned}\boldsymbol{C}_{pp}^k &= \begin{bmatrix} C_{11}^k & C_{12}^k & C_{16}^k \\ C_{12}^k & C_{22}^k & C_{26}^k \\ C_{16}^k & C_{26}^k & C_{66}^k \end{bmatrix} \qquad \boldsymbol{C}_{pn}^k = \begin{bmatrix} 0 & 0 & C_{13}^k \\ 0 & 0 & C_{23}^k \\ 0 & 0 & C_{36}^k \end{bmatrix} \\ \boldsymbol{C}_{np}^k &= \begin{bmatrix} 0 & 0 & 0 \\ 0 & 0 & 0 \\ C_{13}^k & C_{23}^k & C_{36}^k \end{bmatrix} \qquad \boldsymbol{C}_{nn}^k = \begin{bmatrix} C_{55}^k & C_{45}^k & 0 \\ C_{45}^k & C_{44}^k & 0 \\ 0 & 0 & C_{33}^k \end{bmatrix}\end{aligned} \tag{20}$$

The FEM formulation adopts a nine-node shell element based on the Mixed Interpolation of Tensorial Component (MITC) method [199]. The displacement vector becomes

$$\delta\boldsymbol{u}_s = N_j\delta\boldsymbol{u}_{sj}, \qquad \boldsymbol{u}_\tau = N_i\boldsymbol{u}_{\tau i} \qquad i,j = 1,\cdots,9 \tag{21}$$

$\boldsymbol{u}_{\tau i}$ and $\delta\boldsymbol{u}_{sj}$ are the nodal displacement vector and the virtual displacement, respectively. The strain expression becomes

$$\begin{aligned}\boldsymbol{\epsilon}_p &= F_\tau(\boldsymbol{D}_p + \boldsymbol{A}_p)N_i\boldsymbol{u}_{\tau i} \\ \boldsymbol{\epsilon}_n &= F_\tau(\boldsymbol{D}_{n\Omega} - \boldsymbol{A}_n)N_i\boldsymbol{u}_{\tau i} + F_{\tau_{,z}}N_i\boldsymbol{u}_{\tau i}\end{aligned} \tag{22}$$

MITC avoids the membrane and shear locking via a specific interpolation strategy for the strain components on the nine-node shell element, as follows:

$$\begin{aligned}\boldsymbol{\epsilon}_p &= \begin{bmatrix}\epsilon_{\alpha\alpha}\\ \epsilon_{\beta\beta}\\ \epsilon_{\alpha\beta}\end{bmatrix} = \begin{bmatrix} N_{m1} & 0 & 0 \\ 0 & N_{m2} & 0 \\ 0 & 0 & N_{m3}\end{bmatrix}\begin{bmatrix}\epsilon_{\alpha\alpha_{m1}}\\ \epsilon_{\beta\beta_{m2}}\\ \epsilon_{\alpha\beta_{m3}}\end{bmatrix} \\ \boldsymbol{\epsilon}_n &= \begin{bmatrix}\epsilon_{\alpha z}\\ \epsilon_{\beta z}\\ \epsilon_{zz}\end{bmatrix} = \begin{bmatrix} N_{m1} & 0 & 0 \\ 0 & N_{m2} & 0 \\ 0 & 0 & 1\end{bmatrix}\begin{bmatrix}\epsilon_{\alpha z_{m1}}\\ \epsilon_{\beta z_{m2}}\\ \epsilon_{zz_{m3}}\end{bmatrix}\end{aligned} \tag{23}$$

Strains $\epsilon_{\alpha\alpha_{m1}}$, $\epsilon_{\beta\beta_{m2}}$, $\epsilon_{\alpha\beta_{m3}}$, $\epsilon_{\alpha z_{m1}}$, and $\epsilon_{\beta z_{m2}}$ result from Eq. 22 and

$$\begin{aligned}N_{m1} &= [N_{A1}, N_{B1}, N_{C1}, N_{D1}, N_{E1}, N_{F1}] \\ N_{m2} &= [N_{A2}, N_{B2}, N_{C2}, N_{D2}, N_{E2}, N_{F2}] \\ N_{m3} &= [N_P, N_Q, N_R, N_S]\end{aligned} \tag{24}$$

Subscripts m1, m2 and m3 indicate the point groups (A1,B1,C1,D1,E1,F1), (A2,B2,C2,D2,E2,F2), and (P,Q,R,S), respectively, see Fig. 2.
According to d'Alembert's principle in the formulation of Lagrange,

$$\int_{\Omega_k}\int_{A_k} \delta{\boldsymbol{\epsilon}^k}^T\boldsymbol{\sigma}^k H_\alpha^k H_\beta^k d\Omega_k dz + \int_{\Omega_k}\int_{A_k} \rho^k\delta{\boldsymbol{u}^k}^T\ddot{\boldsymbol{u}}^k H_\alpha^k H_\beta^k d\Omega_k dz = 0 \tag{25}$$

Ω_k is the in-plane domain of a layer over the element and A_k is the thickness one. Via the constitutive equations, geometrical, MITC and CUF relations, the following governing equation reads

$$\boldsymbol{m}^k_{\tau isj}\ddot{\boldsymbol{u}}^k_{\tau i} + \boldsymbol{k}^k_{\tau sij}\boldsymbol{u}^k_{\tau i} = 0 \tag{26}$$

$\boldsymbol{k}^k_{\tau sij}$ and $\boldsymbol{m}^k_{\tau sij}$ are 3×3 matrices referred to as the fundamental nucleus of the stiffness and mass matrices, respectively. The components of the nuclei are given in [194]. The assembly over all nodes and elements and the introduction of the harmonic solution leads to the well-known eigenvalue problem,

$$(-\omega^2_n\boldsymbol{M} + \boldsymbol{K})\boldsymbol{U}_n = 0 \tag{27}$$

4 Axiomatic/asymptotic method and best theory diagram, AAM and BTD

The axiomatic/asymptotic method (AAM) is a methodology to evaluate the influence of generalized variables and the accuracy of structural models based on complete or incomplete expansions [22, 23]. In this paper, the axiomatic feature of the procedure considers all the expansions obtainable from the combinations of the full fourth-order expansion, i.e., 2^{15} models. The AAM then obtains asymptotic-like results evaluating the relevance of the unknown variables as problem parameters vary, e.g., thickness, orthotropic ratio, stacking sequence, boundary conditions. The implementation of the AAM may follow various approaches; in this work is as it follows:

1. Definition of parameters such as geometry, boundary conditions, materials, and layer layouts.
2. Axiomatic choice of a starting theory and definition of the starting nodal unknowns. Usually, the starting theory provides 3D-like solutions. The fourth-order, equivalent single layer shell model is the reference model of this paper.
3. The CUF generates the governing equations for the theories considered. In particular, the CUF generates reduced models having combinations of the starting terms as generalized unknowns.
4. For each reduced model, the accuracy evaluation makes use of one or more control parameters; in this paper, the first ten natural frequencies.

Two parameters can identify an expansion, namely, the number of active terms and the error or accuracy provided. The use of two parameters allows the insertion of each expansion in a Cartesian reference frame, as in Fig. 3a. The Best Theory Diagram (BTD) is the curve composed of all models providing the minimum error with the least number of variables, see Fig. 3b. Given the accuracy, models with fewer variables than those on the BTD do not exist. Given the number of variables, models with better accuracy than those on the BTD do not exist.

This paper, for the first time, provides BTD for dynamic problems. To have a single error parameter, the BTD uses the average of the errors as follows:

$$Error = \sum_{i=1}^{10} \frac{f_i / f_i^{N=4}}{10} \tag{28}$$

Where f_i is the i-th frequency from a generic shell model and $f_i^{N=4}$ is the one from the reference solution. As explained in the numerical result section, further control parameters, such as the standard deviation and the Modal Assurance Criterion (MAC), are useful to control the quality of the results.

5 Framework to assess the accuracy of finite elements

The synergistic use of CUF and AAM allows the evaluation of the accuracy of any finite element. The CUF can provide the governing equations of finite elements independently of the expansion adopted to assume the primary variable behavior along the thickness. The AAM provides the BTD as an optimal boundary concerning the accuracy and computational cost. The position of a finite element on the BTD is a form of assessment of its accuracy and computational efficiency. In this paper, the finite elements assessed are those stemming from subsets of the fourth-order model as shown in Table 1. Black and white triangles indicate active and inactive generalized displacement variables, respectively, and DOF the nodal degrees of freedom of the element. N=2, 3, and 4 are the full expansions of the second-, third- and fourth-order. The other three models are well-known from literature and have incomplete expansions. The additional models are the following:

– the First Order Shear Deformation Theory (FSDT) with five DOF,

$$\begin{aligned} u_\alpha &= u_{\alpha_1} + z\, u_{\alpha_2} \\ u_\beta &= u_{\beta_1} + z\, u_{\beta_2} \\ u_z &= u_{z_1} \end{aligned} \tag{29}$$

– a seven DOF model with parabolic transverse displacement, referred to as PTD,

$$\begin{aligned} u_\alpha &= u_{\alpha_1} + z\, u_{\alpha_2} \\ u_\beta &= u_{\beta_1} + z\, u_{\beta_2} \\ u_z &= u_{z_1} + z\, u_{z_2} + z^2\, u_{z_3} \end{aligned} \tag{30}$$

– a nine DOF model with third-order in-plane displacements referred to as TSDT,

$$\begin{aligned} u_\alpha &= u_{\alpha_1} + z\, u_{\alpha_2} + z^2\, u_{\alpha_3} + z^3\, u_{\alpha_4} \\ u_\beta &= u_{\beta_1} + z\, u_{\beta_2} + z^2\, u_{\beta_3} + z^3\, u_{\beta_4} \\ u_z &= u_{z_1} \end{aligned} \tag{31}$$

For the sake of brevity, the comparative analysis focused on the previous models only. The framework can handle any given model including those stemming from layer-wise approaches or non-polynomial expansions [110, 200].

6 Numerical examples

The numerical results focus on spherical shells with geometrical and material features retrieved from [201] and [28]. The shell has a = b and $R_\alpha = R_\beta = R$. The material properties are $E_1/E_2 = 25$, $G_{12}/E_2 = G_{13}/E_2 = 0.5$, $G_{13}/E_2 = 0.2$, $\nu = 0.25$. In all cases, the three constant terms of the expansions, namely, u_{α_1}, u_{β_1} and u_{z1}, are always present in the reduced models. In other words, the combinations considered 12 terms, from linear to fourth-order for a total of 2^{12} models. Such a choice led to a considerable reduction of the computational cost without significant loss of information as previous works proved the presence of constant terms in almost all best models [111]. For the sake of readability, the BTD vertical axis ranges from 5 to 15 as models with 4 or less DOF provide very high errors and are not of practical interest.

6.1 Simply-supported, 0/90/0

The first set of analyses refers to a simply-supported shell with symmetric lamination and various thickness and curvature ratios, a/h, and R/a, respectively. Table 2 presents the first natural frequency from different models including higher- and first-order shear deformation theories, HSDT and FSDT, respectively, CLT, a layer-wise fourth-order model, LD4, and the present equivalent single layer full fourth-order expansion, N=4. The latter provides good accuracy if compared to LD4 and is set as the reference solution to build the BTD. Figure 4 shows the BTD for R/a = 5 and various thicknesses. For instance, in the case of a/h = 10, the 5 DOF BTD provides the first ten natural frequencies with a mean error of 8 %. For the sake of readability of the results, for a/h = 10 and 5, the figure also presents BTD with only N=3. Figure 5 shows the standard deviation (SD) per each BTD and computed on the error distribution. For instance, the 5 DOF BTD model for a/h = 100 has SD = 1.5 %, that is, it provides the first ten natural frequencies with a 1.5 % dispersion on the mean error given in Fig. 4a and equal to 3.2 % for the 5 DOF BTD model. Figure 6 shows the accuracy of all the models stemming from the 2^{12} combinations, that is, each dot on the plot represents a shell finite element and its accuracy in detecting the first ten natural frequencies. The modal assurance criterion (MAC) matrices are shown in Fig. 7 using the first ten natural modes from the nine and eight DOF BTD models and those from the full N=4. Figures 8 and 9 present the BTD and all combination accuracies for a fixed thickness and varying curvature. The terms of BTD models are in Tables 3-7. The last row of each table shows the relevance factor (RF) of the same order variables. The RF is the ratio between the number of active instances and the total number of cases. For instance, concerning Table 3, $RF_0 = 1$ indicates that the zeroth-order terms are always present in the BTD. $RF_4 = 0.27$ because fourth-order variables are in the BTD nine times out of 33 cases. As shown in [111], the RF provides a metric to measure the influence of a set of variables, the higher the RF the higher is the relevance. The numerical results suggest that

- In all cases, 9 DOF are necessary to ensure errors lower than 1 % on the first ten natural frequencies. The thickness ratio is decisive to determine the error ranges of the BTD models. For thin shells, the maximum error with 5 DOF is 3 % whereas, for moderately thick shells it is larger than 8 %. On the other hand, the effect of curvature is less significant.
- In the case of thin shells, of all the models considered for comparison purposes, only the N=3 and FSDT are BTD theories or very close to being BTD. From a/h = 10 and below, N=3 and TSDT are very close to the BTD indicating a predominant role of third-order expansion terms. As indicated previously, the effect of curvature is less significant.
- The standard deviation is smaller than 1 % in all cases with more than 8 DOF. In the case of a/h = 4, SD is larger than 4 % with 7 DOF and below. Such values of SD proves that the choice of the mean error over the first ten natural frequencies is valid as a metric to build the BTD meaning that the BTD models can detect the first ten modal shapes and frequencies with acceptable mean accuracy. The SD curves are similar in all the numerical cases of this paper and, therefore, not reported for the sake of brevity.
- All combination plots present bands with no models indicating accuracy gaps. For instance, for a/h = 100, no models can provide errors in the range of 10-60 %. Such bands are narrow or disappear for thicker shells. Such a phenomenon is consistent with the findings in [111] and is due to the very high relevance of lower-order terms in thin shells, usually up to the first-order. The absence of one of these terms leads to very high errors. On the other hand, for thicker shells, such relevance is weaker with a stronger influence of higher-order terms; therefore, the removal of any terms affect less the accuracy and makes the maximum error smaller.
- MAC is useful to control the quality of the modal shapes from BTD models. The MAC matrices in Fig. 7 refer to the last model with perfect MAC and the first one with some discrepancies, namely, the nine and eight DOF BTD. In all other cases of this section, MAC matrices have no discrepancies meaning that all BTD models can reproduce the first ten modal shapes with high accuracy.
- The analysis of relevance factors from Tables 3-7 shows the increasing importance of third- and fourth-order variables as the thickness increases. Third-order terms tend to become as important as first-order, whereas fourth-order ones tend to equal second-order variables.

6.2 Clamped-free, 0/90/0

The second shell configuration has two non-consecutive edges clamped and the other two free, i.e., the sequence of constrains is clamped/free/clamped/free. Unless otherwise specified, all the other parameters are as in the first case. The aim is to investigate the effect of a different set of geometrical boundary conditions on the BTD. Table 8 shows the first natural frequency compared with a layer-wise model from literature.

As in the previous case, the numerical results focus on BTD plots for various thickness ratios, Fig. 10, the accuracy of reduced models stemming from all 2^{12} combinations, Fig. 11, and the MAC matrix showing that, for the thick case, the 6 DOF BTD cannot detect all ten modes properly, see Fig. 12. Tables 9 and 10 report the BTD models and the RF.
The numerical results show similar tendencies to the simply-supported case. The BTD have similar ranges and the two cases, i.e., simply-supported and clamped-free, share most of the terms composing the best models.

6.3 Simply-supported, 90/0

The last shell configuration considers a different stacking sequence to investigate the effect of an asymmetric lamination on the BTD. All other parameters remain like those of the previous cases.
Table 11 shows the first frequency for the various thickness and curvature ratios considered for the analysis. The results match well those from an ESL with higher-order terms from the literature. Figures 13-16 show the BTD and all combination accuracies, whereas the BTD terms are in Tables 12-15. In all cases, the BTD models detect perfectly all ten modes; therefore, in this section, there are no MAC matrices. The numerical results show that

- The PTD and TSDT are BTD, or very close to the curve, for a/h = 100 and a/h = 10, respectively. FSDT is always BTD but, for a/h = 10, its accuracy is poor. The N=3 is quite close to the BTD, whereas, N=2 is always quite far from it.
- The RF reveals that the second- and fourth-order terms tend to be more relevant than in the 0/90/0 case.

6.4 Analysis of the influence of generalized displacement variables

This section investigates the influence of DOF as problem parameters vary. The methodology makes use of the RF of each DOF as shown in Fig. 17. RF = 1 means that a DOF is in each BTD. For the 0/90/0 case with R/a = 5, u_{β_2} is in every BTD independently of the thickness, whereas, u_{α_2} is in every BTD for a/h = 100 and in the 91 % for a/h = 10 and 5. The analysis considers terms from the first- to the fourth-order, see Figs. 17-20, given that zeroth-order terms are usually always necessary for meaningful accuracy levels. The analysis of each order follows:

- First-order terms. In-plane components are fundamental in all cases with RF close to one. The influence of the transverse term, instead, varies significantly. Such an influence decreases as the thickness increases and is high for the asymmetric lamination.
- Second-order terms. The influence of these terms is, on average, smaller than first-order ones but becomes more significant in the asymmetrical

lamination case. The in-plane components have either little decrements or significant increments of relevance as the thickness increases. As in the previous case, the transverse term influence decreases as the thickness increases.
- Third-order terms. The in-plane components have significant influence in all cases and the relevance increases for thicker shells. The out-of-plane term has a small relevance in all cases.
- Fourth-order terms. These terms are the least influential. The symmetric lamination leads to higher relevances than the asymmetric one.

Further considerations may result using Figs. 21 and 22. These plots are modified versions of Figs. 4a,b and Fig. 15. Each plot shows the displacement field of various structural models with nine and seven DOF to provide insights related to models from the literature. The displacement field on the BTD are also in Tables 3, 4, and 14, 15. The results suggest that

- For thin shells, to improve the accuracy without computational overheads, i.e., moving horizontally and leftward on the BTD diagram, third-order in-plane variables and second-order transverse ones are necessary. In other words, the enhancement of classical theories should give priority to third-order in-plane terms and may neglect second-order ones, whereas, should favor second-order transverse ones.
- For thin shells, best models with decreasing accuracy, i.e., following the BTD down and rightward, keep the second-order transverse term and lose the third-order in-plane ones.
- For thick shells, moving horizontally and leftward on the BTD diagram, complete third-order expansions for the in-plane components gain importance, whereas, the zeroth-order transverse term in enough.
- For thick shells, following the BTD down and rightward, only the third-order in-plane components remain influential.
- The asymmetric lamination case requires displacement fields having a few variations if compared to the symmetric ones. However, for given DOF, the BTD models of the asymmetric case are less accurate than the symmetric ones.

6.5 Summary on the proof of concept

The numerical results exploited the synergy among various methodologies, namely, the Carrera Unified Formulation (CUF) to generate higher-order structural theories, Finite Element Method (FEM) to obtain natural frequencies and modes, axiomatic asymptotic method (AAM) to investigate the influence of generalized displacement variables, and Best Theory Diagrams (BTD) to provide insights on the optimum choice of variables for computational cost minimization. The shell theories evaluated are those stemming from all the subsets given by the combinations of fifteen variables of a full fourth-order model. Such subsets include well-known theories from literature such as the

First- and Third-Order Shear Deformation Theories, FSDT and TSDT, respectively. The metric to evaluate the accuracy of a model is the average error on the first ten natural frequencies with the standard deviation and Modal Assurance Criterion (MAC) as control tools to check the frequency dispersion and modal shape quality. Results refer to various shell configurations concerning thickness, curvature, boundary conditions, and stacking sequence. Models from literature serve as references to verify the framework and draw guidelines for future modeling strategies. Further metrics, referred to as Relevance Factors (RF), proved useful to have an overview of the importance of a variable or order at a glance. The main conclusions are the following:

- The structural features with a predominant role in the determination of the most significant unknown variables are the thickness and the stacking sequence. The influence of curvature and boundary conditions is less evident and require further investigations.
- In most cases, some nine DOF are enough to ensure results as accurate as 99 % of the full fourth-order model.
- The accuracy ranges obtainable by a shell model depends significantly on the thickness. In thin shells, lower-order terms dominate, and their presence allows very accurate results, whereas their absence leads to unacceptable errors. As the thickness increases, higher-order terms gain relevance, and intermediate accuracy levels become viable.
- As a general guideline, the improvement of the shell model without increments of the nodal DOF should favor, first, the third-order in-plane components and, then, the second-order transverse terms. Second- and fourth-order in-plane, third- and fourth-order transverse terms have less relevance.
- The choice of the average error on the first ten frequencies proved to be useful to build reduced models that can predict the global response of the structure under different deformation states. Such a choice improves the validity of the present framework that, in previous works, adopted single or local values under static loads with critical issues regarding generalizations.
- The present framework may serve as a tool to evaluate the accuracy of any structural model and lead to informed decision-making regarding the most convenient sets of generalized variables to use.

7 Considerations on the use of neural networks to assess and develop structural theories

The synergy between CUF and AAM is convenient as a tool for machine learning training [202, 203]. Neural networks (NN) may serve as surrogate models for the fast mapping between given inputs and outputs. In a direct approach, structural theories and problem features are inputs, and accuracies serve as outputs. In an inverse approach, inputs and outputs swap. inputs and outputs swap. For instance, a fourth-order model with inactive terms and h/a

= 0.1 has the following coding:

$$\begin{array}{l} u_\alpha = u_{\alpha_1} + z\, u_{\alpha_2} + z^4\, u_{\alpha_5} \\ u_\beta = u_{\beta_1} + z\, u_{\beta_2} + z^3\, u_{\beta_4} \\ u_z = u_{z_1} + z\, u_{z_2} + z^2\, u_{z_3} \end{array} => [1\,1\,1\,1\,1\,1\,0\,0\,1\,0\,1\,0\,1\,0\,0\,0.1] \tag{32}$$

Where the first fifteen terms of the array refer to the generalized displacement variables and the last one to the thickness ratio. Figure 23 shows the classical approach based on CUF and FE to assess the accuracy and efficiency of a structural theory and the one in which NN substitutes FE. A comparison of the two procedures follows:

- CUF generates the governing FE equations for all the shell theories stemming from subsets of the fourth-order expansions. Given that the expansion has fifteen terms, overall, 2^{15} FE shell models are available. For instance, FSDT is one of these models in which five terms are active - u_{α_1}, u_{β_1}, u_{z1}, u_{α_2}, and u_{β_2} - and ten inactive.
- The FE way runs 2^{15} FE analyses and reports the error and number of active terms of each case in a 2D plot.
- The NN way runs one-tenth of the FE analyses and uses them for training. Then, the 2D plot stems from querying the trained NN with all 2^{15} shell models.
- If a/h is a training variable, and, e.g., three a/h values are available, the overall number of analyses is 3×2^{15}, and the query of the NN includes the shell model and the thickness ratio.

Table 16 reports the typical costs of both procedures. The proper training of NN can partially substitute FE to estimate the accuracy of a shell theory for varying problem features. The primary challenges concern the proper selection of the input features - e.g., thickness, material properties, stacking sequence, boundary conditions - and the significant outputs - e.g., frequencies, stresses. Furthermore, the use of NN for the inverse problem is promising as it would allow the use of a given accuracy to determine the structural theory to use.

8 Conclusions

This paper presented an overview of the existing approaches to develop shell theories for composites and provided a method to assess them. The overview highlighted the seminal importance of the following guidelines:

- Caution is mandatory on the use of classical models available in commercial codes and assuming unstretchable normals and constant shear stress over the thickness. The use of such models may lead to inaccurate results in many meaningful engineering cases, e.g., the presence of local effects are of interest or high-stress gradients, anisotropy and high transverse deformability, and impact problems.

- The Koiter recommendations, i.e., the inclusion of transverse shear and axial stress in refined theories, remain a valuable guideline that should lead the development of shell theories.
- The combined use of the RMVT, third-order expansions and zig-zag distributions, most likely, represents the best accuracy/efficiency trade-off in many cases. The layer-wise option remains mandatory for severe local effects.

To the author's best knowledge, there is no systematic way to assess structural theories. In other words, the only existing approach to evaluate a theory is by comparing its accuracy with other models on a given structural model or by using the asymptotic approach over a given structural or material parameter. The second part of this paper presents the proof of concept of a method that can assess any structural theory and indicate the best models for a given problem concerning the accuracy and computational costs. The main features of the proposed method are

- Given a set of generalized variables, it provides the relevance for each of them and indicates those to retain.
- Via the Best Theory Diagrams (BTD), the assessment of any structural theory is possible concerning the best accuracy available with the same number of DOF or the minimum number of DOF required to meet the same accuracy.
- The proposed method has coding features that are very promising in a machine learning scenario. The training of neural networks may ease the simultaneous assessment over the primary variables, the problem characteristics, and the accuracy. Also, it may lead to surrogate models requiring a fraction of the computational costs of classical FE, accepting accuracy requirements as the input and providing the structural theory to use as the output.

References

1. A. L. Cauchy. Sur l'équilibre et le mouvement d'une plaque solide. *Exercises de Matematique*, 3:328–355, 1828.
2. S. D. Poisson. Memoire sur l'équilibre et le mouvement des corps elastique. *Mem. Acad. Sci.*, 1829.
3. A.E.H. Love. *The Mathematical Theory of Elasticity.* Cambridge Univ Press, fourth edition, 1927.
4. G. Kirchhoff. Uber das gleichgewicht und die bewegung einer elastischen scheibe. *Journal fur reins und angewandte Mathematik*, 40:51–88, 1850.
5. E. Reissner. The effect of transverse shear deformation on the bending of elastic plates. *Journal of Applied Mechanics*, 12:69–76, 1945.
6. R.D. Mindlin. Influence of rotatory inertia and shear in flexural motions of isotropic elastic plates. *Journal of Applied Mechanics*, 18:1031–1036, 1951.

7. S.A. Ambartsumian. Nontraditional theories of shells and plates. *Applied Mechanics Reviews*, 55(5):R35–R44, 2002.
8. E. Carrera. Theories and finite elements for multilayered, anisotropic, composite plates and shells. *Archives of Computational Methods in Engineering*, 9(2):87–140, 2002.
9. S.G. Lekhnitskii. Strength calculation of composite beams. *Vestnik inzhen i tekhnikov*, 9, 1935.
10. F.B. Hildebrand, E. Reissner, and G.B. Thomas. Notes on the foundations of the theory of small displacements of orthotropic shells. *NACA TN-1833*, 1949.
11. W.T. Koiter. A consistent first approximation in the general theory of thin elastic shells. *Proceedings of Symposium on the Theory of Thin Elastic Shells, August 1959, North-Holland, Amsterdam*, pages 12–23, 1959.
12. S.A. Ambartsumian. Contributions to the theory of anisotropic layered shells. *Applied Mechanics Reviews*, 15:245–249, 1962.
13. N.J. Pagano. Exact solutions for composite laminates in cylindrical bending. *Journal of Composite Materials*, 3(3):398–411, 1969.
14. A.W. Leissa. Vibration of shells. *NASA-SP-288*, LC-77-186367, 1973.
15. E.I. Grigolyuk and G.M. Kulikov. General directions of the development of theory of shells. *Mechanics of Composite Materials*, 24(287–298), 1988.
16. K. Kapania. A review on the analysis of laminated shells. *ASME Journal of Pressure Vessel Technology*, 111(2):88–96, 1989.
17. A.K. Noor and W.S. Burton. Assessment of computational models for multilayered composite shells. *Applied Mechanics Reviews*, 43(4):67–97, 1989.
18. M. Touratier. A generalization of shear deformation theories for axisymmetric multilayered shells. *International Journal of Solids and Structures*, 29(11):1379 – 1399, 1992.
19. V.V. Vasil'Ev and S.A. Lur'E. On refined theories of beams, plates, and shells. *Journal of Composite Materials*, 26(4):546–557, 1992.
20. J. N. Reddy and D. H. Robbins. Theories and computational models for composite laminates. *Applied Mechanics Reviews*, 47(6):147–165, 1994.
21. K. Washizu. *Variational Methods in Elasticity and Plasticity*. Pergamon, Oxford, 1968.
22. E. Carrera and M. Petrolo. Guidelines and recommendation to construct theories for metallic and composite plates. *AIAA Journal*, 48(12):2852–2866, 2010.
23. E. Carrera and M. Petrolo. On the effectiveness of higher-order terms in refined beam theories. *Journal of Applied Mechanics*, 78, 2011.
24. A.L. Gol'denweizer. *Theory of thin elastic shells*. International Series of Monograph in Aeronautics and Astronautics. Pergamon Press, New York, 1961.
25. P. Cicala. *Systematic approximation approach to linear shell theory*. Levrotto e Bella, Torino, 1965.

26. J.N. Reddy. Exact solutions of moderately thick laminated shells. *Journal of Engineering Mechanics*, 110(5):794–809, 1984.
27. J.G. Ren. Exact solutions for laminated cylindrical shells in cylindrical bending. *Composites Science and Technology*, 29(3):169 – 187, 1987.
28. J.N. Reddy and C.F. Liu. A higher-order shear deformation theory of laminated elastic shells. *International Journal of Engineering Science*, 23(3):319 – 330, 1985.
29. C.P. Wu and C.C. Liu. Stress and displacement of thick doubly curved laminated shells. *Journal of Engineering Mechanics*, 120(7):1403–1428, 1994.
30. A.W. Leissa and J.D. Chang. Elastic deformation of thick, laminated composite shells. *Composite Structures*, 35(2):153 – 170, 1996.
31. X.P. Shu. A refined theory of laminated shells with higher-order transverse shear deformation. *International Journal of Solids and Structures*, 34(6):673 – 683, 1997.
32. X. Wang, C. Wang, and Z.Y. Yu. An analytic method for interlaminar stress in a laminated cylindrical shell. *Mechanics of Advanced Materials and Structures*, 9(2):119–131, 2002.
33. A.S. Oktem and R.A. Chaudhuri. Fourier analysis of thick cross-ply Levy type clamped doubly-curved panels. *Composite Structures*, 80(4):489 – 503, 2007.
34. A.K. Noor and P.L. Rarig. Three-dimensional solutions of laminated cylinders. *Computer Methods in Applied Mechanics and Engineering*, 3(3):319 – 334, 1974.
35. T K Varadan and K Bhaskar. Bending of laminated orthotropic cylindrical shells - an elasticity approach. *Composite Structures*, 17:141–156, 1991.
36. J. Fan and J. Zhang. Analytical solutions for thick, doubly curved, laminated shells. *Journal of Engineering Mechanics*, 118(7):1338–1356, 1992.
37. A. Bhimaraddi and K. Chandrashekhara. Three-dimensional elasticity solution for static response of simply supported orthotropic cylindrical shells. *Composite Structures*, 20(4):227 – 235, 1992.
38. C.P. Wu and J.Y. Lo. Three-dimensional elasticity solutions of laminated annular spherical shells. *Journal of Engineering Mechanics*, 126(8):882–885, 2000.
39. P. Kumari and S. Kar. Static behavior of arbitrarily supported composite laminated cylindrical shell panels: An analytical 3D elasticity approach. *Composite Structures*, 207:949 – 965, 2019.
40. R.K. Khare, V. Rode, A.K. Garg, and S.P. John. Higher-order closed-form solutions for thick laminated sandwich shells. *Journal of Sandwich Structures & Materials*, 7(4):335–358, 2005.
41. A.K. Garg, R.K. Khare, and T. Kant. Higher-order closed-form solutions for free vibration of laminated composite and sandwich shells. *Journal of Sandwich Structures & Materials*, 8(3):205–235, 2006.
42. H. Biglari and A.A. Jafari. High-order free vibrations of doubly-curved sandwich panels with flexible core based on a refined three-layered theory.

Composite Structures, 92(11):2685 – 2694, 2010.
43. E. Asadi, W. Wang, and M.S. Qatu. Static and vibration analyses of thick deep laminated cylindrical shells using 3d and various shear deformation theories. *Composite Structures*, 94(2):494 – 500, 2012.
44. S. Hosseini-Hashemi, S.R. Atashipour, M. Fadaee, and U.A. Girhammar. An exact closed-form procedure for free vibration analysis of laminated spherical shell panels based on Sanders theory. *Archive of Applied Mechanics*, 82(7):985–1002, 2012.
45. J.L. Mantari and C. Guedes Soares. Analysis of isotropic and multilayered plates and shells by using a generalized higher-order shear deformation theory. *Composite Structures*, 94(8):2640 – 2656, 2012.
46. C. Hwu, H.W. Hsu, and Y.H. Lin. Free vibration of composite sandwich plates and cylindrical shells. *Composite Structures*, 171:528 – 537, 2017.
47. G. Jin, T. Ye, X. Ma, Y. Chen, Z. Su, and X. Xie. A unified approach for the vibration analysis of moderately thick composite laminated cylindrical shells with arbitrary boundary conditions. *International Journal of Mechanical Sciences*, 75:357 – 376, 2013.
48. G. Jin, T. Ye, Y. Chen, Z. Su, and Y. Yan. An exact solution for the free vibration analysis of laminated composite cylindrical shells with general elastic boundary conditions. *Composite Structures*, 106:114 – 127, 2013.
49. T. Ye, G. Jin, Y. Chen, X. Ma, and Z. Su. Free vibration analysis of laminated composite shallow shells with general elastic boundaries. *Composite Structures*, 106:470 – 490, 2013.
50. Y. Qu and G. Meng. Dynamic analysis of composite laminated and sandwich hollow bodies of revolution based on three-dimensional elasticity theory. *Composite Structures*, 112:378 – 396, 2014.
51. G. Jin, T. Ye, and S. Shi. Three-dimensional vibration analysis of isotropic and orthotropic open shells and plates with arbitrary boundary conditions. *Shock and Vibration*, 2015, 2015.
52. H. Li, F. Pang, X. Wang, Y. Du, and H. Chen. Free vibration analysis for composite laminated doubly-curved shells of revolution by a semi analytical method. *Composite Structures*, 201:86 – 111, 2018.
53. R. Zhong, J. Tang, A. Wang, C. Shuai, and Q. Wang. An exact solution for free vibration of cross-ply laminated composite cylindrical shells with elastic restraint ends. *Computers and Mathematics with Applications*, 77(3):641 – 661, 2019.
54. A.L. Poore, A. Barut, and E. Madenci. Free vibration of laminated cylindrical shells with a circular cutout. *Journal of Sound and Vibration*, 312(1):55 – 73, 2008.
55. M. Shakouri and M.A. Kouchakzadeh. Analytical solution for vibration of generally laminated conical and cylindrical shells. *International Journal of Mechanical Sciences*, 131-132:414 – 425, 2017.
56. S.G.P. Castro and M.V. Donadon. Assembly of semi-analytical models to address linear buckling and vibration of stiffened composite panels with debonding defect. *Composite Structures*, 160:232 – 247, 2017.

57. M.H. Kargarnovin and M. Hashemi. Free vibration analysis of multilayered composite cylinder consisting fibers with variable volume fraction. *Composite Structures*, 94(3):931 – 944, 2012.
58. A.V. Lopatin and E.V. Morozov. Fundamental frequency of the laminated composite cylindrical shell with clamped edges. *International Journal of Mechanical Sciences*, 92:35 – 43, 2015.
59. M. Nasihatgozar, S.M.R. Khalili, and K.M. Fard. General equations for free vibrations of thick doubly curved sandwich panels with compressible and incompressible core using higher order shear deformation theory. *Steel and Composite Structures*, 24(2):151–176, 2017.
60. C.P. Wu and K.H. Chiu. Rmvt-based meshless collocation and element-free galerkin methods for the quasi-3d free vibration analysis of multilayered composite and fgm plates. *Composite Structures*, 93(5):1433 – 1448, 2011.
61. A.H. Sofiyev. Application of the first order shear deformation theory to the solution of free vibration problem for laminated conical shells. *Composite Structures*, 188:340 – 346, 2018.
62. A.V. Singh and V. Kumar. Vibration of laminated shallow shells on quadrangular boundary. *Journal of Aerospace Engineering*, 9(2):52–57, 1996.
63. A.V. Singh and L. Shen. Free vibration of open circular cylindrical composite shells with point supports. *Journal of Aerospace Engineering*, 18(2):120–128, 2005.
64. X. Zhao, K.M. Liew, and T.Y. Ng. Vibration analysis of laminated composite cylindrical panels via a meshfree approach. *International Journal of Solids and Structures*, 40(1):161 – 180, 2003.
65. T. Ye, G. Jin, Z. Su, and X. Jia. A unified Chebyshev–Ritz formulation for vibration analysis of composite laminated deep open shells with arbitrary boundary conditions. *Archive of Applied Mechanics*, 84:441–471, 2017.
66. G. Jin, T. Ye, X. Jia, and S. Gao. A general Fourier solution for the vibration analysis of composite laminated structure elements of revolution with general elastic restraints. *Composite Structures*, 109:150 – 168, 2014.
67. X. Song, Q. Han, and J. Zhai. Vibration analyses of symmetrically laminated composite cylindrical shells with arbitrary boundaries conditions via Rayleigh–Ritz method. *Composite Structures*, 134:820 – 830, 2015.
68. F. Pang, H. Li, H. Chen, and Y. Shan. Free vibration analysis of combined composite laminated cylindrical and spherical shells with arbitrary boundary conditions. *Mechanics of Advanced Materials and Structures*, 2019.
69. G. Jin, Z. Su, T. Ye, and X. Jia. Three-dimensional vibration analysis of isotropic and orthotropic conical shells with elastic boundary restraints. *International Journal of Mechanical Sciences*, 89:207 – 221, 2014.
70. C. Yang, G. Jin, Y. Zhang, and Z. Liu. A unified three-dimensional method for vibration analysis of the frequency-dependent sandwich shallow shells with general boundary conditions. *Applied Mathematical Mod-*

elling, 66:59 – 76, 2019.
71. A.V. Singh. Free vibration analysis of deep doubly curved sandwich panels. *Computers and Structures*, 73(1):385 – 394, 1999.
72. M. Hemmatnezhad, G.H. Rahimi, M. Tajik, and F. Pellicano. Experimental, numerical and analytical investigation of free vibrational behavior of GFRP-stiffened composite cylindrical shells. *Composite Structures*, 120:509 – 518, 2015.
73. X. Xie, H. Zheng, and G. Jin. Integrated orthogonal polynomials based spectral collocation method for vibration analysis of coupled laminated shell structures. *International Journal of Mechanical Sciences*, 98:132 – 143, 2015.
74. Y. Qu, H. Hua, and G. Meng. A domain decomposition approach for vibration analysis of isotropic and composite cylindrical shells with arbitrary boundaries. *Composite Structures*, 95:307 – 321, 2013.
75. Y. Qu, X. Long, S. Wu, and G. Meng. A unified formulation for vibration analysis of composite laminated shells of revolution including shear deformation and rotary inertia. *Composite Structures*, 98:169 – 191, 2013.
76. J. Guo, D. Shi, Q. Wang, J. Tang, and C. Shuai. Dynamic analysis of laminated doubly-curved shells with general boundary conditions by means of a domain decomposition method. *International Journal of Mechanical Sciences*, 138-139:159 – 186, 2018.
77. A. Alibeigloo. Static and vibration analysis of axi-symmetric angle-ply laminated cylindrical shell using state space differential quadrature method. *International Journal of Pressure Vessels and Piping*, 86(11):738 – 747, 2009.
78. H.V. Lakshminarayana and K. Dwarakanath. Free vibration characteristics of cylindrical shells made of composite materials. *Journal of Sound and Vibration*, 154(3):431 – 439, 1992.
79. J. Zhu. Free vibration analysis of multilayered composite plates and shells with the natural approach. *Computer Methods in Applied Mechanics and Engineering*, 130(1):133 – 149, 1996.
80. N.S. Bardell, J.M. Dunsdon, and R.S. Langley. Free and forced vibration analysis of thin, laminated, cylindrically curved panels. *Composite Structures*, 38(1):453 – 462, 1997.
81. T. Park, K. Kim, and S. Han. Linear static and dynamic analysis of laminated composite plates and shells using a 4-node quasi-conforming shell element. *Composites Part B: Engineering*, 37(2):237 – 248, 2005.
82. H. Nguyen-Van, N. Mai-Duy, and T. Tran-Cong. Free vibration analysis of laminated plate/shell structures based on fsdt with a stabilized nodal-integrated quadrilateral element. *Journal of Sound and Vibration*, 313(1):205 – 223, 2008.
83. H. Nguyen-Van, N. Mai-Duy, W. Karunasena, and T. Tran-Cong. Buckling and vibration analysis of laminated composite plate/shell structures via a smoothed quadrilateral flat shell element with in-plane rotations. *Computers and Structures*, 89(7):612 – 625, 2011.

84. D. Chakravorty, J.N. Bandyopadhyay, and P.K. Sinha. Finite element free vibration analysis of point supported laminated composite cylindrical shells. *Journal of Sound and Vibration*, 181(1):43 – 52, 1995.
85. K.S.S. Ram and T.S. Babu. Free vibration of composite spherical shell cap with and without a cutout. *Computers and Structures*, 80(23):1749 – 1756, 2002.
86. S.C. Han, S. Choi, and S.Y. Chang. Nine-node resultant-stress shell element for free vibration and large deflection of composite laminates. *Journal of Aerospace Engineering*, 19(2):103–120, 2006.
87. S. Jayasankar, S. Mahesh, S. Narayanan, and Chandramouli Padmanabhan. Dynamic analysis of layered composite shells using nine node degenerate shell elements. *Journal of Sound and Vibration*, 299(1):1 – 11, 2007.
88. I.F. Pinto Correia, C.M. Mota Soares, C.A. Mota Soares, and J. Herskovits. Analysis of laminated conical shell structures using higher order models. *Composite Structures*, 62(3):383 – 390, 2003.
89. R.K. Khare, T. Kant, and A.K. Garg. Free vibration of composite and sandwich laminates with a higher-order facet shell element. *Composite Structures*, 65(3):405 – 418, 2004.
90. R.K. Khare, A.K. Garg, and T. Kant. Free vibration of sandwich laminates with two higher-order shear deformable facet shell element models. *Journal of Sandwich Structures & Materials*, 7(3):221–244, 2005.
91. A. Kumar, P. Bhargava, and A. Chakrabarti. Vibration of laminated composite skew hypar shells using higher order theory. *Thin-Walled Structures*, 63:82 – 90, 2013.
92. S.N. Thakur and C. Ray. An accurate C0 finite element model of moderately thick and deep laminated doubly curved shell considering cross sectional warping. *Thin-Walled Structures*, 94:384 – 393, 2015.
93. S.N. Thakur, C. Ray, and S. Chakraborty. A new efficient higher-order shear deformation theory for a doubly curved laminated composite shell. *Acta Mechanica*, 228(1):69–87, 2017.
94. F. Dau, O. Polit, and M.Touratier. An efficient C^1 finite element with continuity requirements for multilayered/sandwich shell structures. *Computers and Structures*, 82(23):1889 – 1899, 2004.
95. T. Yamamoto, T. Yamada, and K. Matsui. A quadrilateral shell element with degree of freedom to represent thickness–stretch. *Computational Mechanics*, 59(4):625–646, 2017.
96. R.R. Paccola, M.S.M. Sampaio, and H.B. Coda. Continuous stress distribution following transverse direction for fem orthotropic laminated plates and shells. *Applied Mathematical Modelling*, 40(15):7382 – 7409, 2016.
97. H. Parisch. A critical survey of the 9-node degenerated shell element with special emphasis on thin shell application and reduced integration. *Computer Methods in Applied Mechanics and Engineering*, 20(3):323 – 350, 1979.
98. K.Y. Sze, L.Q. Yao, and T.H.H. Pian. An eighteen-node hybrid-stress solid-shell element for homogenous and laminated structures. *Finite El-*

ements in Analysis and Design, 38(4):353 – 374, 2002.
99. M. Fiolka and A. Matzenmiller. On the resolution of transverse stresses in solid-shells with a multi-layer formulation. *Communications in Numerical Methods in Engineering*, 23(4):313–326, 2007.
100. S. Shiri and H. Naceur. Analysis of thin composite structures using an efficient hex-shell finite element. *Journal of Mechanical Science and Technology*, 27(12):3755–3763, 2013.
101. K. Rah, W. Van Paepegem, A.M. Habraken, and J. Degrieck. A mixed solid-shell element for the analysis of laminated composites. *International Journal for Numerical Methods in Engineering*, 89(7):805–828, 2012.
102. Y.W. Kwon. Analysis of laminated and sandwich composite structures using solid-like shell elements. *Applied Composite Materials*, 20(4):355–373, 2013.
103. G.M. Kulikov and S.V. Plotnikova. Exact geometry four-node solid-shell element for stress analysis of functionally graded shell structures via advanced SaS formulation. *Mechanics of Advanced Materials and Structures*, In Press.
104. M. Jabareen and E. Mtanes. A solid-shell Cosserat point element for the analysis of geometrically linear and nonlinear laminated composite structures. *Finite Elements in Analysis and Design*, 142:61 – 80, 2018.
105. L. Leonetti and H. Nguyen-Xuan. A mixed edge-based smoothed solid-shell finite element method (mes-fem) for laminated shell structures. *Composite Structures*, 208:168 – 179, 2019.
106. Y. Ko, Y. Lee, P.S. Lee, and K.J. Bathe. Performance of the MITC3+ and MITC4+ shell elements in widely-used benchmark problems. *Computers and Structures*, 193:187–206, 2017.
107. G. Rama, D. Marinkovic, and M. Zehn. High performance 3-node shell element for linear and geometrically nonlinear analysis of composite laminates. *Composites Part B: Engineering*, 151:118–126, 2018.
108. T. Ho-Nguyen-Tan and H.G. Kim. A new strategy for finite-element analysis of shell structures using trimmed quadrilateral shell meshes: A paving and cutting algorithm and a pentagonal shell element. *International Journal for Numerical Methods in Engineering*, 114(1):1–27, 2018.
109. K Wisniewski and E Turska. Improved nine-node shell element MITC9i with reduced distortion sensitivity. *Computational Mechanics*, 62(3):499–523, 2018.
110. E. Carrera, M. Cinefra, A. Lamberti, and M. Petrolo. Results on best theories for metallic and laminated shells including layer-wise models. *Composite Structures*, 126:285–298, 2015.
111. M. Petrolo and E. Carrera. Best theory diagrams for multilayered structures via shell finite elements. *Advanced Modeling and Simulation in Engineering Science*, 6(4):1–23, 2019.
112. E. Carrera, F. Miglioretti, and M. Petrolo. Computations and evaluations of higher-order theories for free vibration analysis of beams. *Journal of Sound and Vibration*, 331(19):4269 – 4284, 2012.

113. E. Carrera. Theories and finite elements for multilayered plates and shells: a unified compact formulation with numerical assessment and benchmarking. *Archives of Computational Methods in Engineering*, 10(3):216–296, 2003.
114. Y. Vetyukov. Hybrid asymptotic-direct approach to the problem of finite vibrations of a curved layered strip. *Acta Mechanica*, 223(2):371–385, 2012.
115. H. Kraus. *Thin elastic shells*. 1967.
116. J.N. Reddy. A Simple Higher-Order Theory for Laminated Composite Plates. *Journal of Applied Mechanics*, 51(4):745–752, 1984.
117. M. Endo. An alternative first-order shear deformation concept and its application to beam, plate and cylindrical shell models. *Composite Structures*, 146:50–61, 2016.
118. Q. Wang, D. Shao, and B. Qin. A simple first-order shear deformation shell theory for vibration analysis of composite laminated open cylindrical shells with general boundary conditions. *Composite Structures*, 184:211 – 232, 2018.
119. N.N. Huang. Influence of shear correction factors in the higher-order shear deformation laminated shell theory. *International Journal of Solids and Structures*, 31:1263–1277, 1994.
120. S.N. Thakur, C. Ray, and S. Chakraborty. A new efficient higher-order shear deformation theory for a doubly curved laminated composite shell. *Acta Mechanica*, 228(1):69–87, 2017.
121. S.N. Thakur, C. Ray, and S. Chakraborty. Response sensitivity analysis of laminated composite shells based on higher-order shear deformation theory. *Archive of Applied Mechanics*, 88(8):1429–1459, 2018.
122. C.P. Wu and C.C. Liu. Stress and displacement of thick doubly curved laminated shells. *Journal of Engineering Mechanics*, 120(7):1403–1428, 1994.
123. C.P. Wu and C.C. Liu. A local high-order deformable theory for thick laminated cylindrical shells. *Composite Structures*, 29(1):69 – 87, 1994.
124. P.H. Shah and R.C. Batra. Stress singularities and transverse stresses near edges of doubly curved laminated shells using tsndt and stress recovery scheme. *European Journal of Mechanics - A/Solids*, 63:68 – 83, 2017.
125. P.H. Shah and R.C. Batra. Stretching and bending deformations due to normal and shear tractions of doubly curved shells using third-order shear and normal deformable theory. *Mechanics of Advanced Materials and Structures*, 25(15-16):1276–1296, 2018.
126. S.M.R. Khalili, S. Tafazoli, and K.M. Fard. Free vibrations of laminated composite shells with uniformly distributed attached mass using higher order shell theory including stiffness effect. *Journal of Sound and Vibration*, 330(26):6355 – 6371, 2011.
127. P. Desai and T. Kant. On numerical analysis of axisymmetric thick circular cylindrical shells based on higher order shell theories by segmentation method. *Journal of Sandwich Structures & Materials*, 17(2):130–169,

2015.
128. O. Rabinovitch and Y. Frostig. High-order analysis of unidirectional sandwich panels with flat and generally curved faces and a "soft" core. *Journal of Sandwich Structures & Materials*, 3(2):89–116, 2001.
129. Y. Frostig, C.N. Phan, and G.A. Kardomateas. Free vibration of unidirectional sandwich panels, part i: Compressible core. *Journal of Sandwich Structures & Materials*, 15(4):377–411, 2013.
130. D Punera and T Kant. Elastostatics of laminated and functionally graded sandwich cylindrical shells with two refined higher order models. *Composite Structures*, 182:505–523, 2017.
131. W. Zhen and C. Wanji. A global-local higher order theory for multilayered shells and the analysis of laminated cylindrical shell panels. *Composite Structures*, 84(4):350 – 361, 2008.
132. C. Ossadzow and M. Touratier. An improved shear-membrane theory for multilayered shells. *Composite Structures*, 52(1):85 – 95, 2001.
133. A.J.M. Ferreira, E. Carrera, M. Cinefra, C.M.C. Roque, and O. Polit. Analysis of laminated shells by a sinusoidal shear deformation theory and radial basis functions collocation, accounting for through-the-thickness deformations. *Composites Part B: Engineering*, 42(5):1276 – 1284, 2011.
134. J.L. Mantari, A.S. Oktem, and C. Guedes Soares. Bending and free vibration analysis of isotropic and multilayered plates and shells by using a new accurate higher-order shear deformation theory. *Composites Part B: Engineering*, 43(8):3348 – 3360, 2012.
135. H.T. Thai, T.P. Vo, T.Q. Bui, and T.K. Nguyen. A quasi-3d hyperbolic shear deformation theory for functionally graded plates. *Acta Mechanica*, 225(3):951–964, 2014.
136. A.S. Sayyad and Y.M. Ghugal. Static and free vibration analysis of laminated composite and sandwich spherical shells using a generalized higher-order shell theory. *Composite Structures*, 219:129 – 146, 2019.
137. E. Carrera. Historical review of zig-zag theories for multilayered plates and shells. *Applied Mechanics Review*, 56:287–308, 2003.
138. S.A. Ambartsumian. On a general theory of anisotropic shells. *Journal of Applied Mathematics and Mechanics*, 22(2):305 – 319, 1958.
139. H Murakami. Laminated composite plate theory with improved in-plane response. *Journal of Applied Mechanics*, 53:661–666, 1986.
140. Ya.M. Grigorenko and A.T. Vasilenko. Taking account of nonuniformity of transverse displacement deformation in thickness in layered shells. *Soviet Applied Mechanics*, 13(10):989–994, 1977.
141. A.O. Rasskazov. Theory of multilayer orthotropic shallow shells. *Soviet Applied Mechanics*, 12(11):1131–1136, 1976.
142. V.G. Piskunov and A.A. Rasskazov. Investigation of stresss-trained state of tapered orthotropic shells and plates on the basis of second order shear theory. *International Applied Mechanics*, 34(8):798 – 806, 1998.
143. J.M. Whitney. The effect of transverse shear deformation on the bending of laminated plates. *Journal of Composite Materials*, 3(3):534–547, 1969.

144. B.K. Rath and Y.C. Das. Vibration of layered shells. *Journal of Sound and Vibration*, 28(4):737 – 757, 1973.
145. K.P. Soldatos and T. Timarci. A unified formulation of laminated composite, shear deformable, five-degrees-of-freedom cylindrical shell theories. *Composite Structures*, 25(1):165 – 171, 1993.
146. A. Kumar, A. Chakrabarti, and P. Bhargava. Vibration of laminated composites and sandwich shells based on higher order zigzag theory. *Engineering Structures*, 56:880 – 888, 2013.
147. A. Kumar, A. Chakrabarti, and P. Bhargava. Finite element analysis of laminated composite and sandwich shells using higher order zigzag theory. *Composite Structures*, 106:270 – 281, 2013.
148. A Ahmed and S Kapuria. A four-node facet shell element for laminated shells based on the third order zigzag theory. *Composite Structures*, 158(1):112–127, 2016.
149. H.B. Coda, R.R. Paccola, and R. Carrazedo. Zig-Zag effect without degrees of freedom in linear and non linear analysis of laminated plates and shells. *Composite Structures*, 161:32–50, 2017.
150. T.M. Hsu and J.T. Wang. Rotationally symmetric vibrations of orthotropic layered cylindrical shells. *Journal of Sound and Vibration*, 16(4):473 – 487, 1971.
151. Y.K. Cheung and C.I. Wu. Free vibrations of thick, layered cylinders having finite length with various boundary conditions. *Journal of Sound and Vibration*, 24(2):189 – 200, 1972.
152. D.H. Robbins Jr. and J.N. Reddy. Modelling of thick composites using a layerwise laminate theory. *International Journal for Numerical Methods in Engineering*, 36(4):655–677, 1993.
153. J.N. Reddy. *Mechanics of laminated composite plates and shells. Theory and Analysis*. CRC Press, 2^{nd} edition, 2004.
154. A. Dasgupta and K.H. Huang. A layer-wise analysis for free vibrations of thick composite spherical panels. *Journal of Composite Materials*, 31(7):658–671, 1997.
155. M. Yaqoob Yasin and S. Kapuria. An efficient layerwise finite element for shallow composite and sandwich shells. *Composite Structures*, 98:202 – 214, 2013.
156. Y. Guo and M. Ruess. A layerwise isogeometric approach for NURBS-derived laminate composite shells. *Composite Structures*, 124:300 – 309, 2015.
157. K. Khan, B.P. Patel, and Y. Nath. Dynamic characteristics of bimodular laminated panels using an efficient layerwise theory. *Composite Structures*, 132:759 – 771, 2015.
158. M. Marjanović and D. Vuksanović. Free vibrations of laminated composite shells using the rotation-free plate elements based on reddy's layerwise discontinuous displacement model. *Composite Structures*, 156:320 – 332, 2016.
159. G.M. Kulikov and S.V. Plotnikova. Strong sampling surfaces formulation for layered shells. *International Journal of Solids and Structures*, 121:75

– 85, 2017.
160. D.H. Li and F. Zhang. Full extended layerwise method for the simulation of laminated composite plates and shells. *Computers and Structures*, 187:101–113, 2017.
161. K. Naumenko and V.A. Eremeyev. A layer-wise theory of shallow shells with thin soft core for laminated glass and photovoltaic applications. *Composite Structures*, 178:434–446, 2017.
162. E. Reissner. On a mixed variational theorem and on shear deformable plate theory. *International Journal for Numerical Methods in Engineering*, 23(2):193–198, 1986.
163. E. Reissner. On a certain mixed variational theorem and on laminated elastic shell theory. In I. Elishakoff and H. Irretier, editors, *Refined Dynamical Theories of Beams, Plates and Shells and Their Applications*, pages 17–27, Berlin, Heidelberg, 1987. Springer Berlin Heidelberg.
164. K. Bhaskar and T.K. Varadan. Reissner's new mixed variational principle applied to laminated cylindrical shells. *Journal of Pressure Vessel Technology*, 114(1):115 – 119, 1992.
165. E. Carrera. Developments, ideas and evaluations based upon the Reissner's mixed variational theorem in the modeling of multilayered plates and shells. *Applied Mechanics Review*, 54:301–329, 2001.
166. O. A. Fettahlioglu and C. R. Steele. Asymptotic solutions for orthotropic non-homogeneous shells of revolution. *Journal of Applied Mechanics*, 44:753–758, 1974.
167. V.L. Berdichevsky. Variational-asymptotic method of shell theory construction. *PMM*, 43:664–667, 1979.
168. C. Lee and D.H. Hodges. Dynamic variational-asymptotic procedure for laminated composite shells—part I: Low-frequency vibration analysis. *Journal of Applied Mechanics*, 76(1), 2008.
169. C.Y. Lee and D.H. Hodges. Asymptotic construction of a dynamic shell theory: Finite-element-based approach. *Thin-Walled Structures*, 47(3):256 – 270, 2009.
170. A. Louhghalam, T. Igusa, and M. Tootkaboni. Dynamic characteristics of laminated thin cylindrical shells: Asymptotic analysis accounting for edge effect. *Composite Structures*, 112:22 – 37, 2014.
171. C.P. Wu, J.Q. Tarn, and S.M. Chi. Three-dimensional analysis of doubly curved laminated shells. *Journal of Engineering Mechanics*, 122(5):391–401, 1996.
172. C.P. Wu, J.Q. Tarn, and P.Y. Chen. Refined asymptotic theory of doubly curved laminated shells. *Journal of Engineering Mechanics*, 123(12):1238–1246, 1997.
173. C.P. Wu and Y.C. Hung. Asymptotic theory of laminated circular conical shells. *International Journal of Engineering Science*, 37(8):977 – 1005, 1999.
174. C.P. Wu and Y.W. Chi. Asymptotic solutions of laminated composite shallow shells with various boundary conditions. *Acta Mechanica*, 132(1):1–18, 1999.

175. N.K. Akhmedov and A.H. Sofiyev. Asymptotic analysis of three-dimensional problem of elasticity theory for radially inhomogeneous transversally-isotropic thin hollow spheres. *Thin-Walled Structures*, 139:232 – 241, 2019.
176. P.G. Ciarlet and V. Lods. Asymptotic analysis of linearly elastic shells. i. justification of membrane shell equations. *Archive for Rational Mechanics and Analysis*, 136(2):119–161, 1996.
177. M. Dauge, E. Faou, and Z. Yosibash. *Plates and Shells: Asymptotic Expansions and Hierarchical Models*, pages 1–39. American Cancer Society, 2017.
178. P.E. Tovstik. On the asymptotic nature of approximate models of beams, plates, and shells. *Vestnik St. Petersburg University: Mathematics*, 40(3):188–192, 2007.
179. Y. Vetyukov, E. Staudigl, and M. Krommer. Hybrid asymptotic–direct approach to finite deformations of electromechanically coupled piezoelectric shells. *Acta Mechanica*, 229(2):953–974, 2018.
180. E. Prulière. 3d simulation of laminated shell structures using the proper generalized decomposition. *Composite Structures*, 117:373 – 381, 2014.
181. B. Bognet, A. Leygue, and F. Chinesta. Separated representations of 3d elastic solutions in shell geometries. *Advanced Modeling and Simulation in Engineering Sciences*, 1(1):4, 2014.
182. P. Vidal, L. Gallimard, and O. Polit. Shell finite element based on the proper generalized decomposition for the modeling of cylindrical composite structures. *Computers and Structures*, 132:1 – 11, 2014.
183. P. Vidal, L. Gallimard, and O. Polit. Multiresolution strategies for the modeling of composite shell structures based on the variable separation method. *International Journal for Numerical Methods in Engineering*, 117(7):778–799, 2019.
184. E. Carrera. The effects of shear deformation and curvature on buckling and vibrations of cross-ply laminated composite shells. *Journal of Sound and Vibrations*, 150(3):405–433, 1991.
185. E. Carrera. A study of transverse normal stress effect on vibration of multilayered plates and shells. *Journal of Sound and Vibration*, 225(5):803 – 829, 1999.
186. E. Carrera. A Reissner's mixed variational theorem applied to vibration analysis of multilayered shell. *Journal of Applied Mechanics*, 66(1):69–78, 1999.
187. E. Carrera. Multilayered shell theories accounting for layerwise mixed description, Part 1: Governing equations. *AIAA Journal*, 37(9):1107–1116, 1999.
188. E. Carrera. Multilayered shell theories accounting for layerwise mixed description, Part 2: Numerical evaluations. *AIAA Journal*, 37(9):1117–1124, 1999.
189. B. Brank and E. Carrera. Multilayered shell finite element with interlaminar continuous shear stresses: a refinement of the Reissner–Mindlin formulation. *International Journal for Numerical Methods in Engineer-*

ing, 48(6):843–874, 2000.
190. B. Brank and E. Carrera. A family of shear-deformable shell finite elements for composite structures. *Computers and Structures*, 76(1):287 – 297, 2000.
191. E. Carrera. On the use of the Murakami's zig-zag function in the modeling of layered plates and shells. *Computers and Structures*, 82(7):541 – 554, 2004.
192. E. Carrera and G. Giunta. Exact, hierarchical solutions for localized loadings in isotropic, laminated, and sandwich shells. *Journal of Pressure Vessel Technology*, 131(4), 2009.
193. M. Cinefra and E. Carrera. Shell finite elements with different through-the-thickness kinematics for the linear analysis of cylindrical multilayered structures. *International Journal for Numerical Methods in Engineering*, 93(2):160–182, 2013.
194. E. Carrera, M. Cinefra, M. Petrolo, and E. Zappino. *Finite Element Analysis of Structures through Unified Formulation*. John Wiley & Sons, Chichester, 2014.
195. M. Cinefra, C. Chinosi, L. Della Croce, and E. Carrera. Refined shell finite elements based on RMVT and MITC for the analysis of laminated structures. *Composite Structures*, 113:492–497, 2014.
196. M. Cinefra and S. Valvano. A variable kinematic doubly-curved MITC9 shell element for the analysis of laminated composites. *Mechanics of Advanced Materials and Structures*, 23(11):1312–1325, 2016.
197. E. Carrera, A. Pagani, and S. Valvano. Shell elements with through-the-thickness variable kinematics for the analysis of laminated composite and sandwich structures. *Composites Part B: Engineering*, 111:294 – 314, 2017.
198. G. Li, E. Carrera, M. Cinefra, A.G. de Miguel, A. Pagani, and E. Zappino. An adaptable refinement approach for shell finite element models based on node-dependent kinematics. *Composite Structures*, 210:1 – 19, 2019.
199. K.J. Bathe and E.N. Dvorkin. A formulation of general shell elements—the use of mixed interpolation of tensorial components. *International Journal for Numerical Methods in Engineering*, 22(3):697–722, 1986.
200. M. Petrolo and A. Lamberti. Axiomatic/asymptotic analysis of refined layer-wise theories for composite and sandwich plates. *Mechanics of Advanced Materials and Structures*, 23(1):28–42, 2016.
201. M. Cinefra. Free-vibration analysis of laminated shells via refined MITC9 elements. *Mechanics of Advanced Materials and Structures*, 23(9):937–947, 2016.
202. M. Petrolo and E. Carrera. On the use of neural networks to evaluate performances of shell models for composites. *Advanced Modeling and Simulation in Engineering Science*, In Press.
203. M. Petrolo and E. Carrera. Best structural theories for free vibrations of sandwich composites via machine learning. In *Proceedings of the ASME 2019 International Mechanical Engineering Congress and Expo-*

sition IMECE2019.

Figures

Fig. 1 Shell geometry.

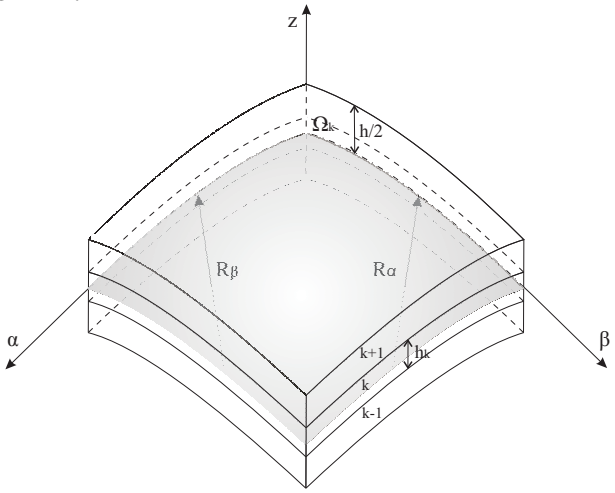

Fig. 2 MITC9 tying points.

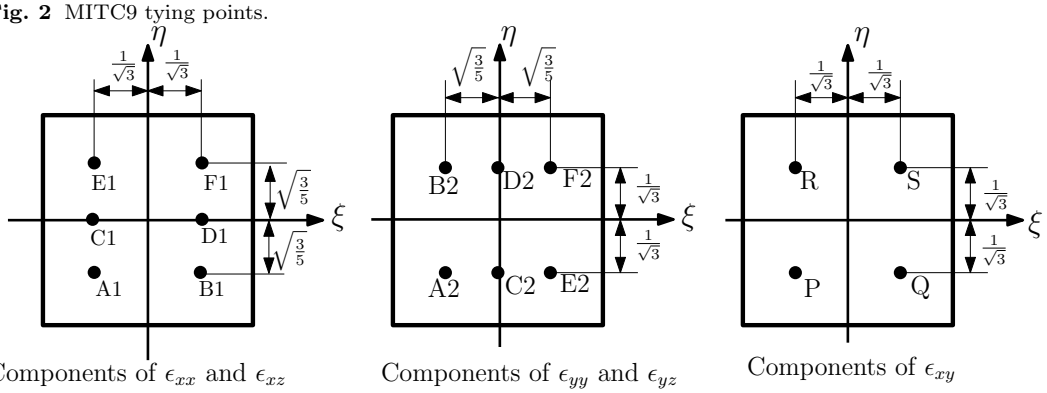

Components of ϵ_{xx} and ϵ_{xz} Components of ϵ_{yy} and ϵ_{yz} Components of ϵ_{xy}

Fig. 3 Representation of FE in a 2D Cartesian reference frame and an example of BTD.

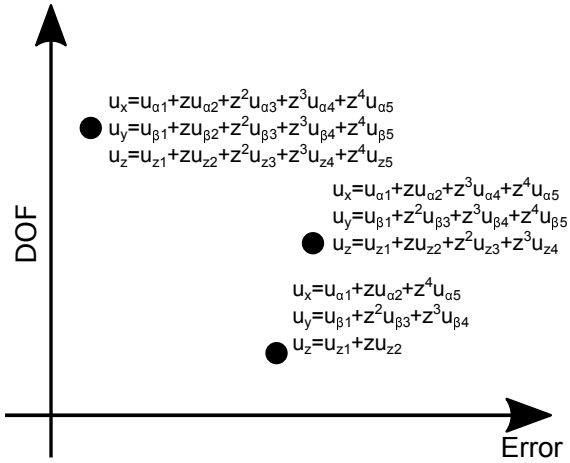

(a) Three shell theories

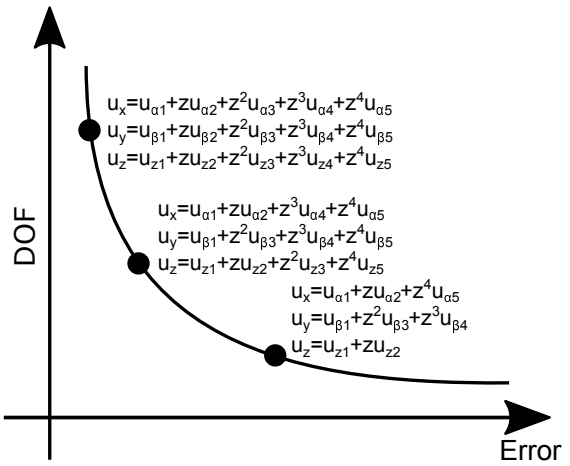

(b) BTD

Fig. 4 BTD for 0/90/0, R/a = 5.

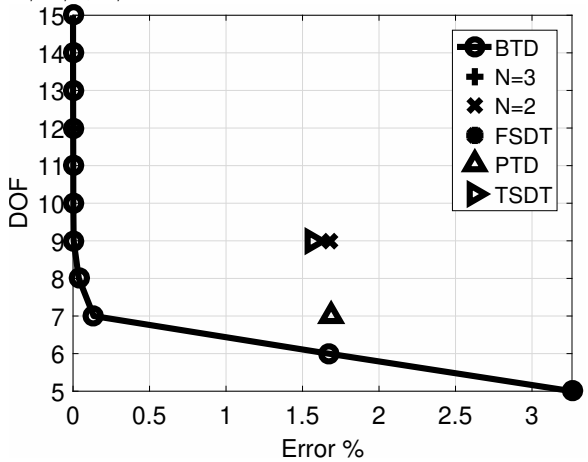

(a) a/h = 100

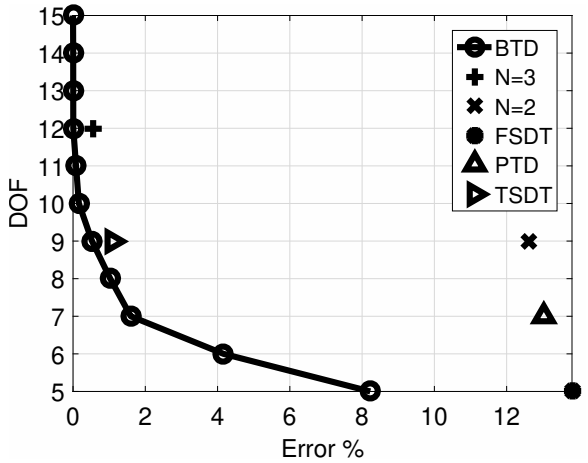

(b) a/h = 10

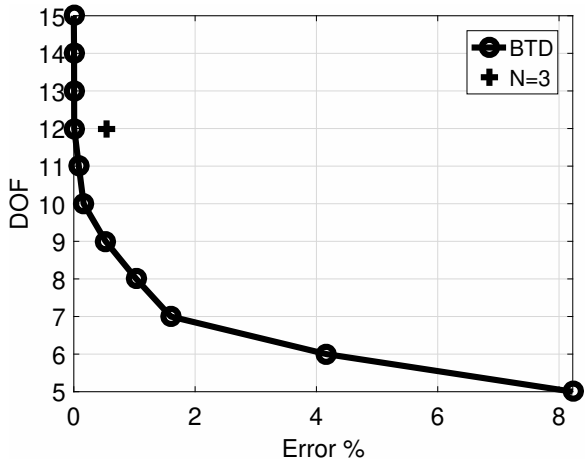

(c) a/h = 10 with N = 3

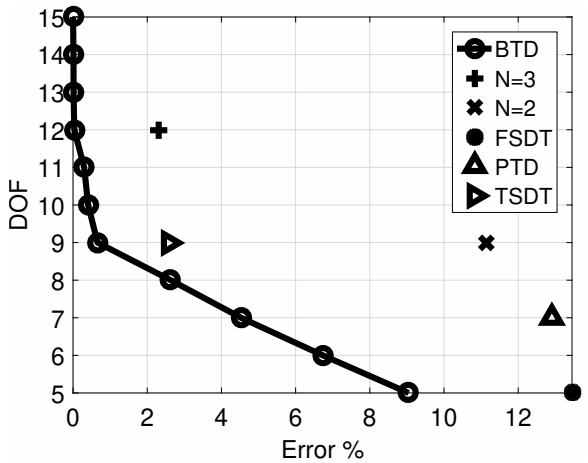

Fig. 5 STD for 0/90/0, R/a = 5.

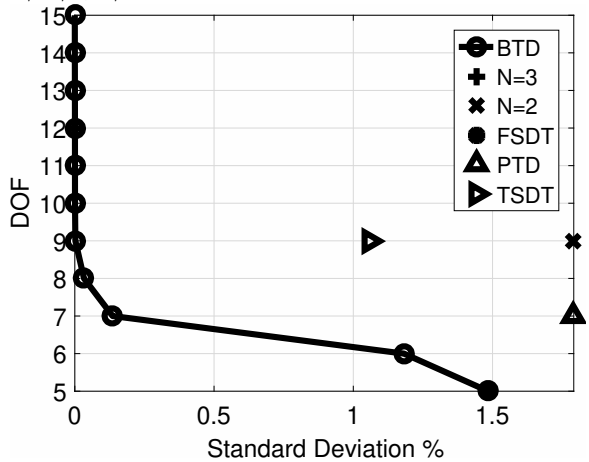

(a) a/h = 100

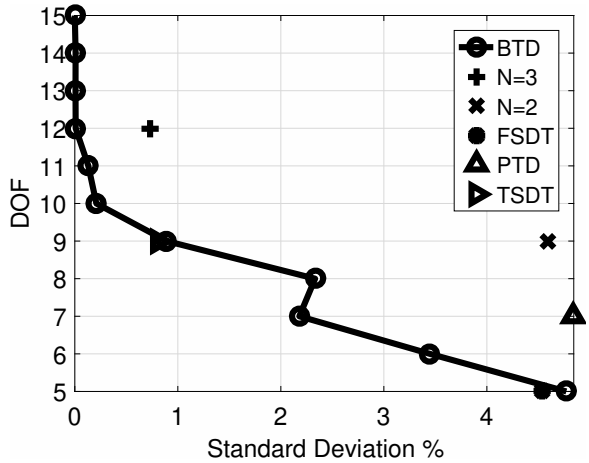

(b) a/h = 10

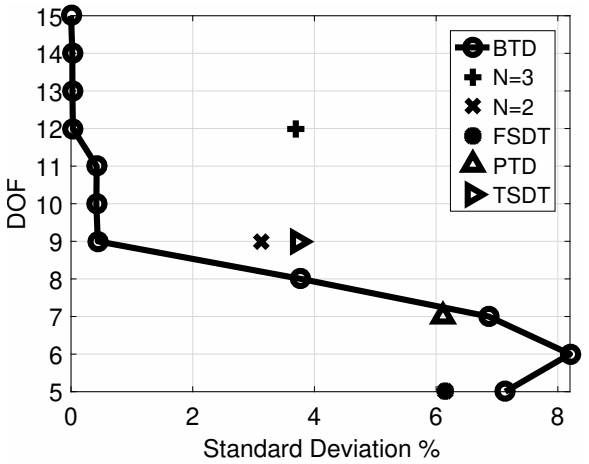

(c) a/h = 5

Fig. 6 All combinations for 0/90/0, R/a = 5.

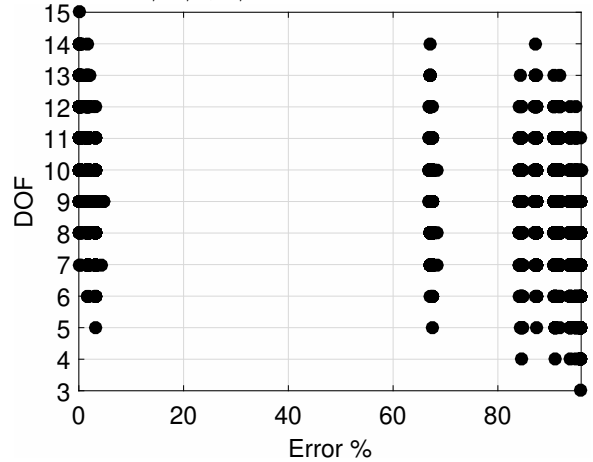

(a) a/h = 100

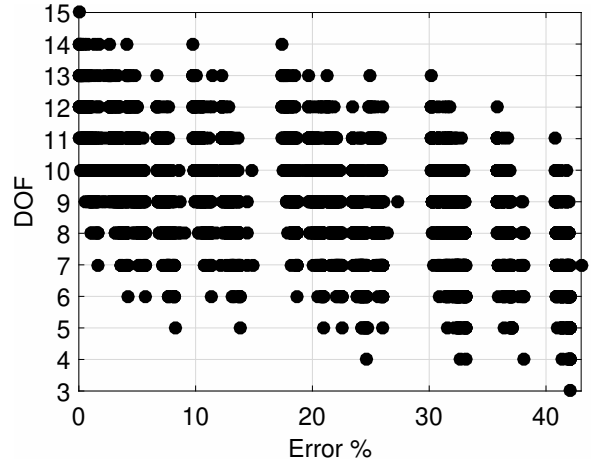

(b) a/h = 10

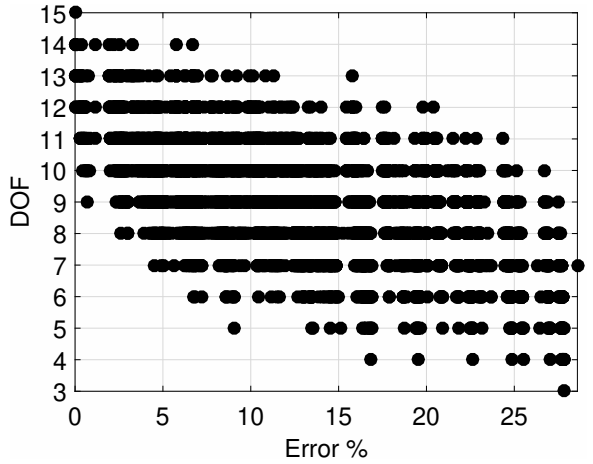

(c) a/h = 5

Fig. 7 MAC for 0/90/0, R/a = 5, a/h = 5.

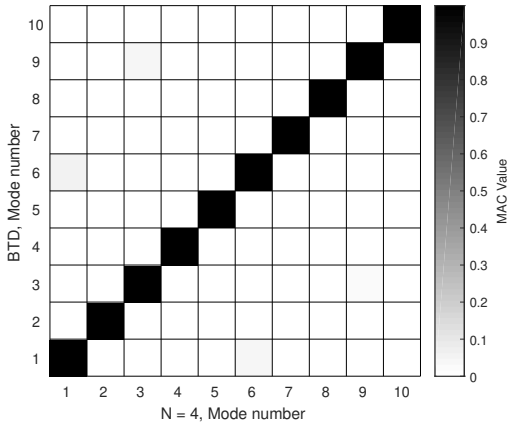

(a) 9 DOF BTD

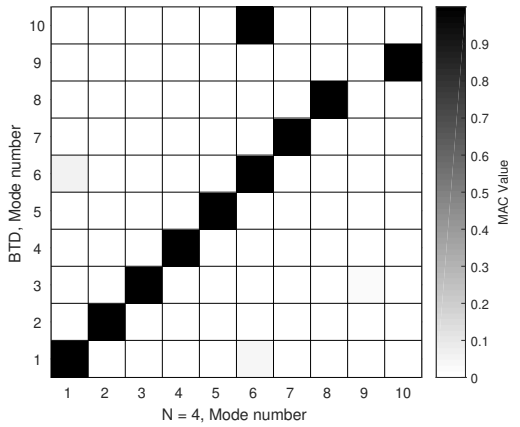

(b) 8 DOF BTD

Fig. 8 BTD for 0/90/0, a/h = 10.

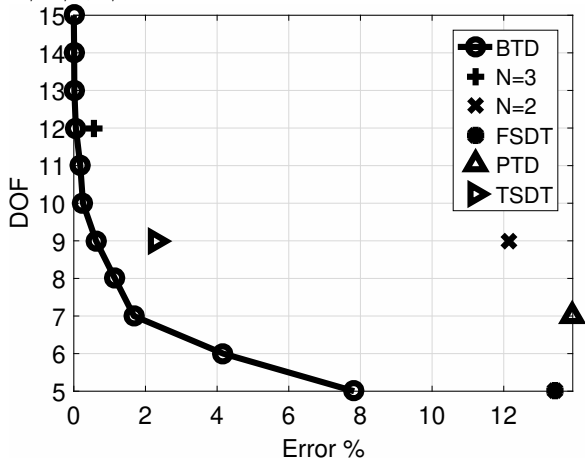

(a) R/a = 2

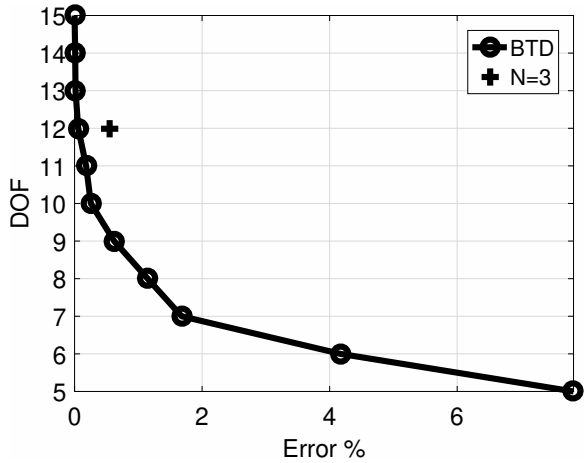

(b) R/a = 2 with N = 3

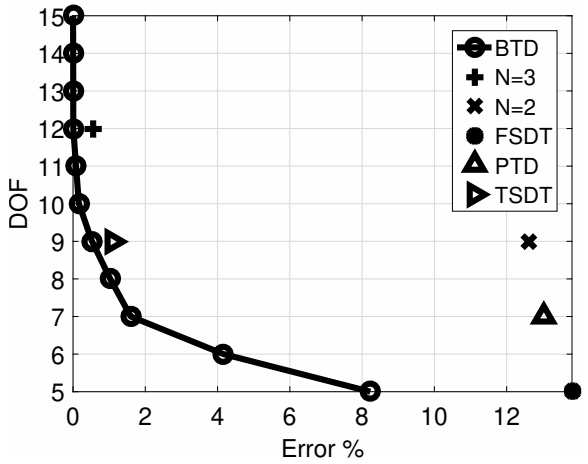

(c) R/a = 5

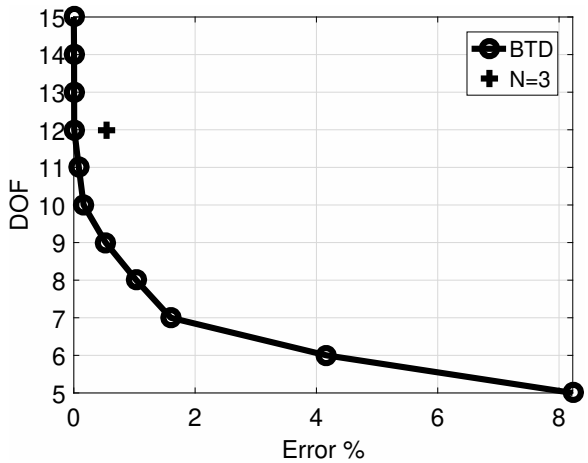

Fig. 9 All combinations for 0/90/0, a/h = 10.

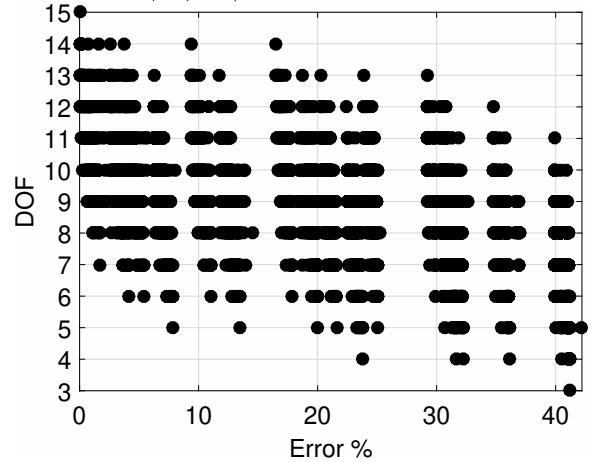

(a) R/a = 2

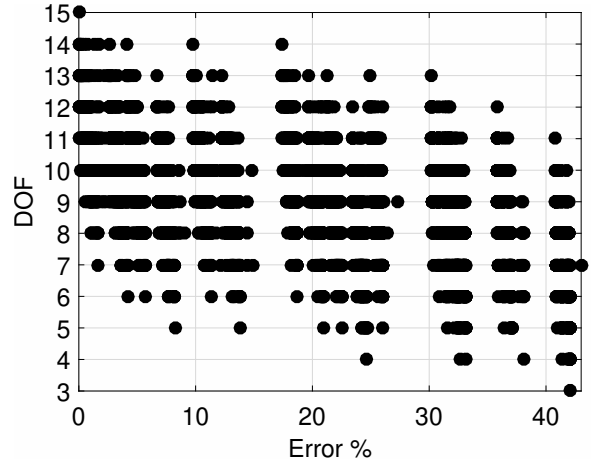

(b) R/a = 5

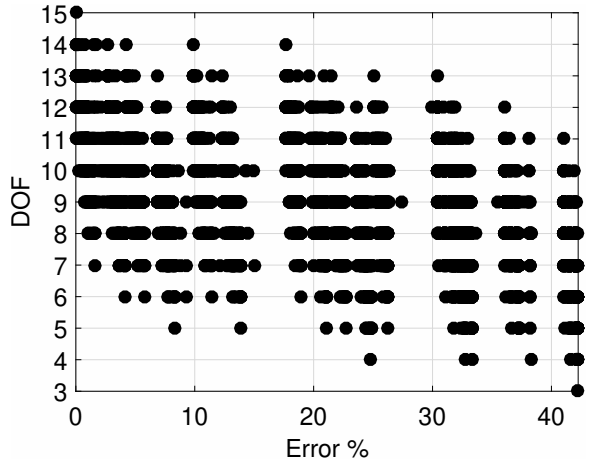

(c) Plate

Fig. 10 BTD for 0/90/0, clamped-free, R/a = 10.

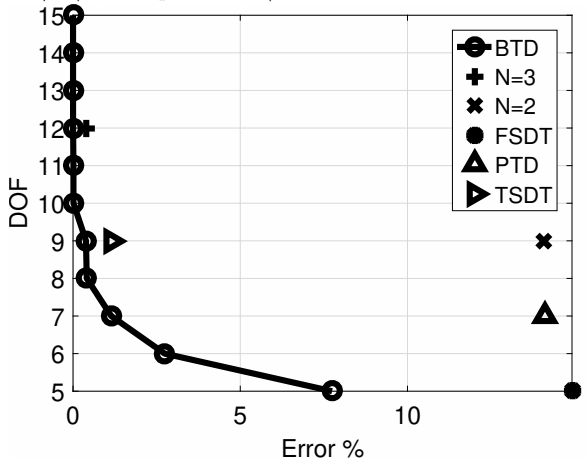

(a) a/h = 20

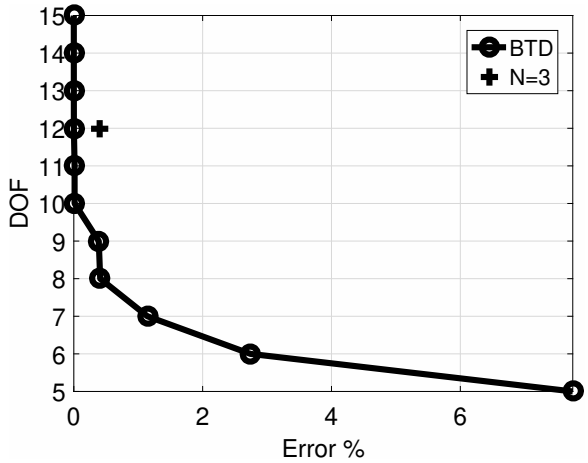

(b) a/h = 20 with N = 3

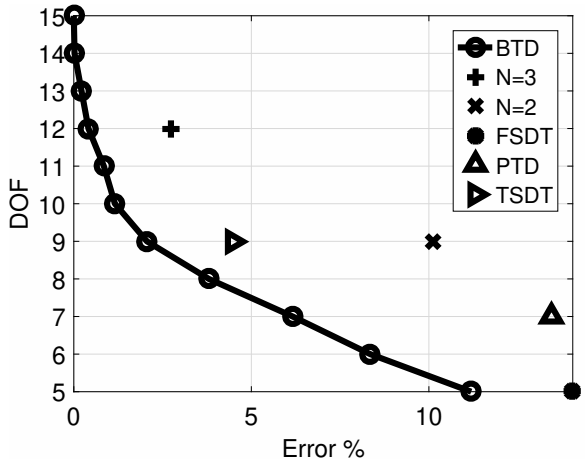

(c) a/h = 4

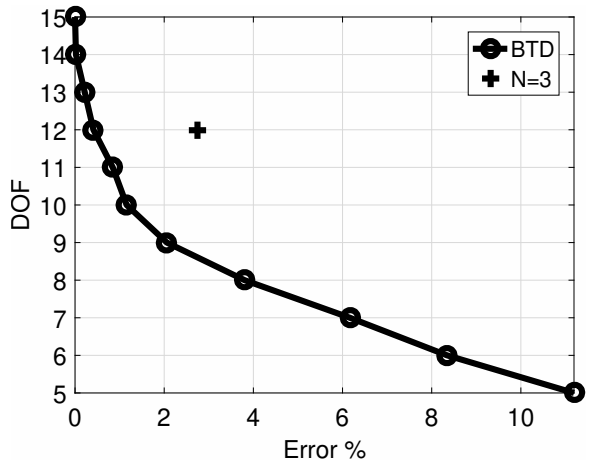

Fig. 11 All combinations for 0/90/0, clamped-free, R/a = 10.

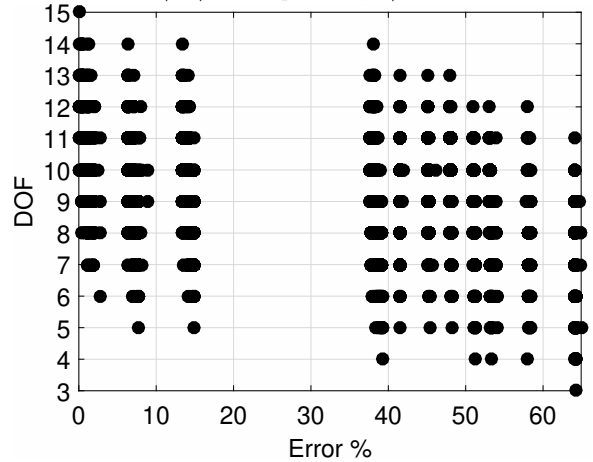

(a) a/h = 20

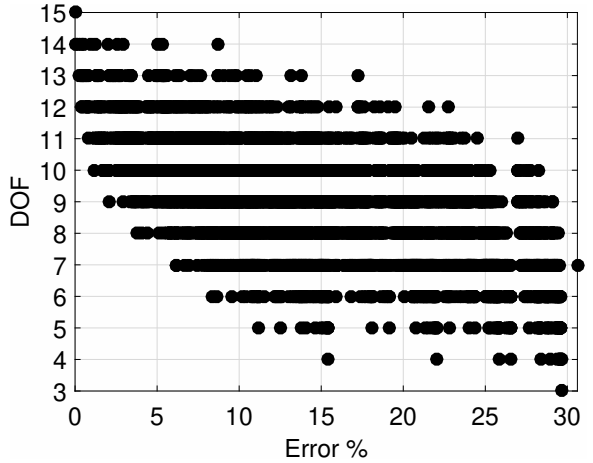

(b) a/h = 4

Fig. 12 MAC for 0/90/0, clamped-free, R/a = 10, a/h = 4.

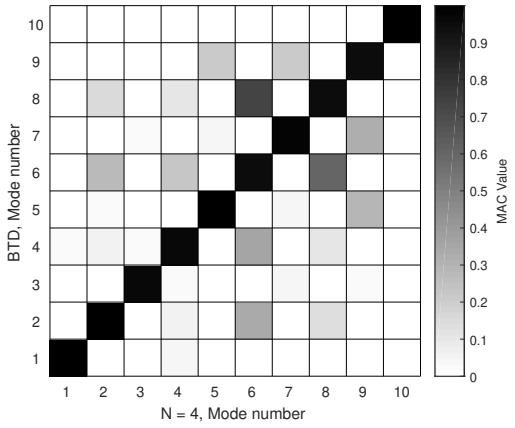

(a) 7 DOF BTD

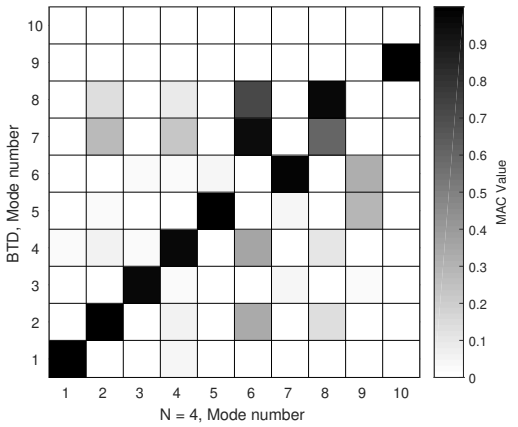

(b) 6 DOF BTD

Fig. 13 BTD for 90/0, R/a = 5.

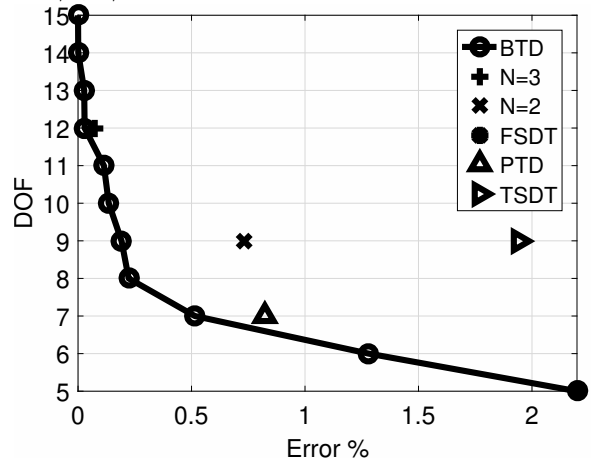

(a) a/h = 100

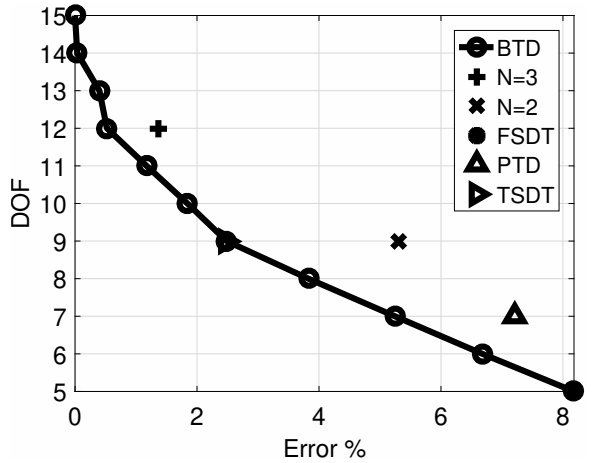

(b) a/h = 10

Fig. 14 All combinations for 90/0, R/a = 5.

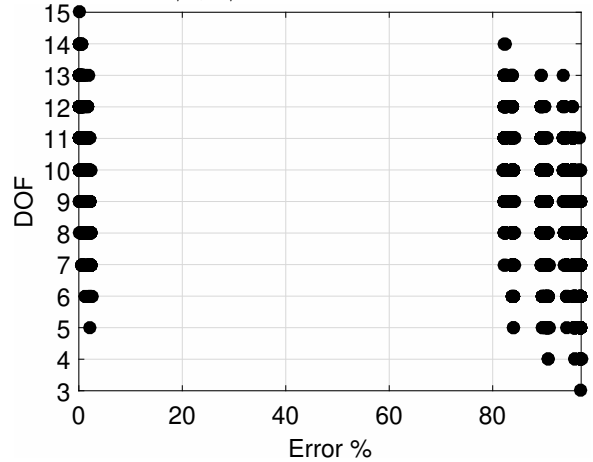

(a) a/h = 100

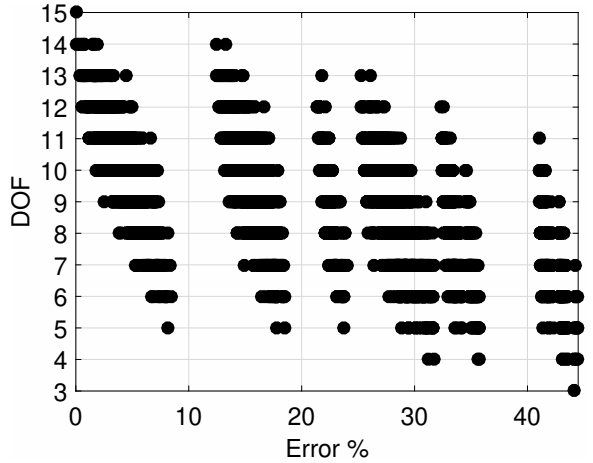

(b) a/h = 10

Fig. 15 BTD for 90/0, R/a = 20.

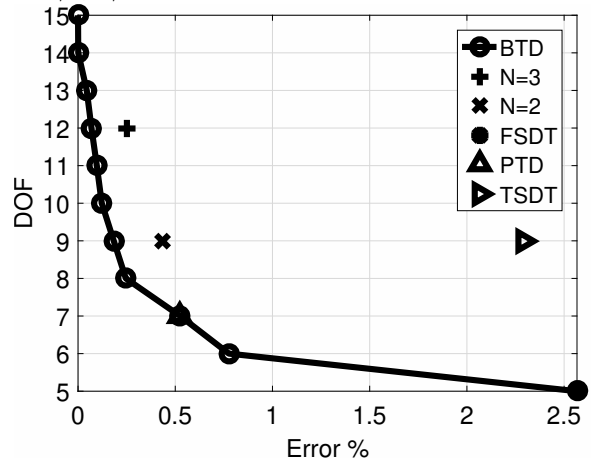

(a) a/h = 100

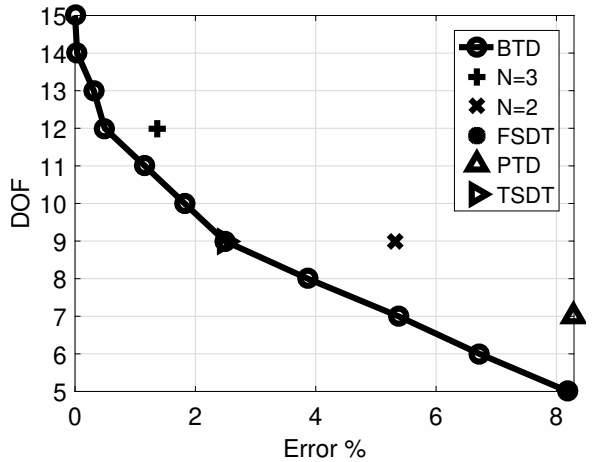

(b) a/h = 10

Fig. 16 All combinations for 90/0, R/a = 20.

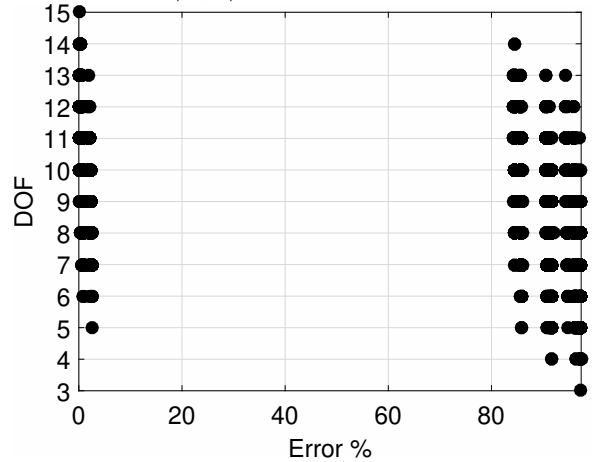

(a) a/h = 100

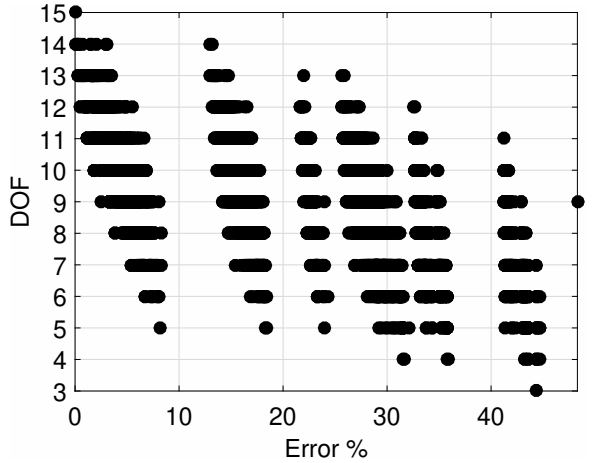

(b) a/h = 10

Fig. 17 RP for first-order DOF.

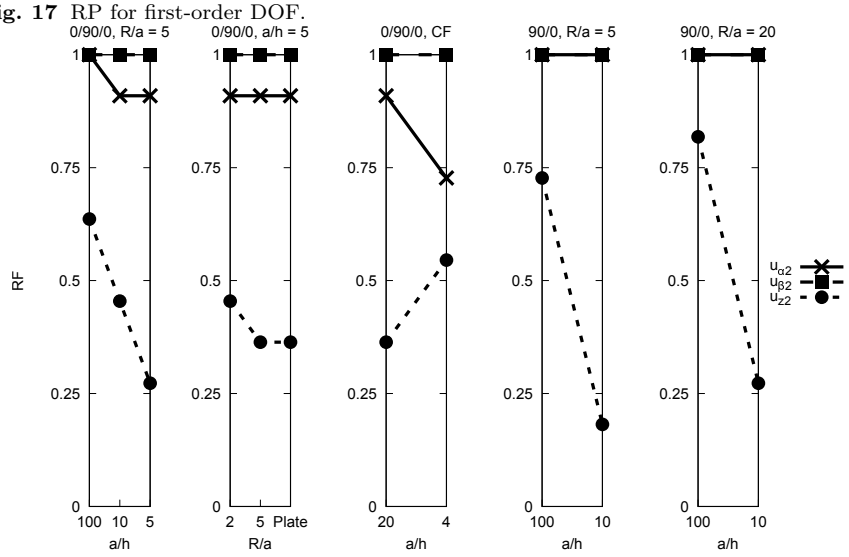

Fig. 18 RP for second-order DOF.

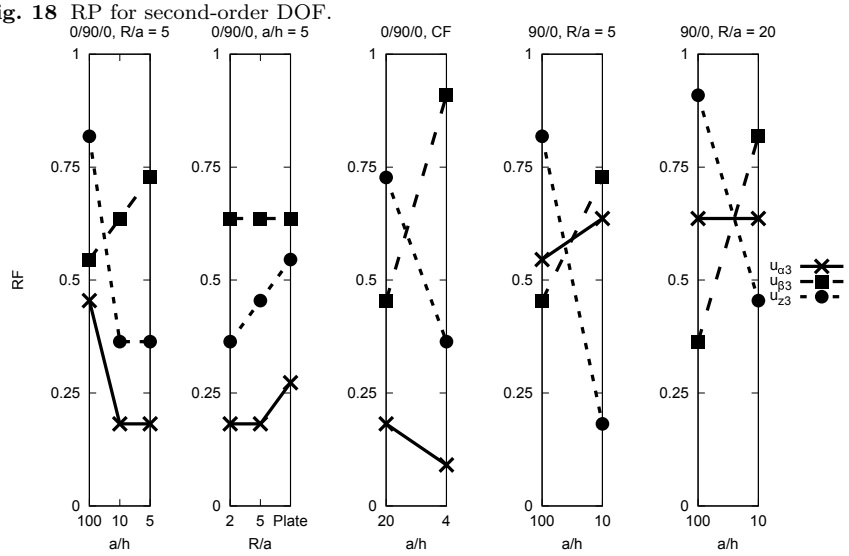

Fig. 19 RP for third-order DOF.

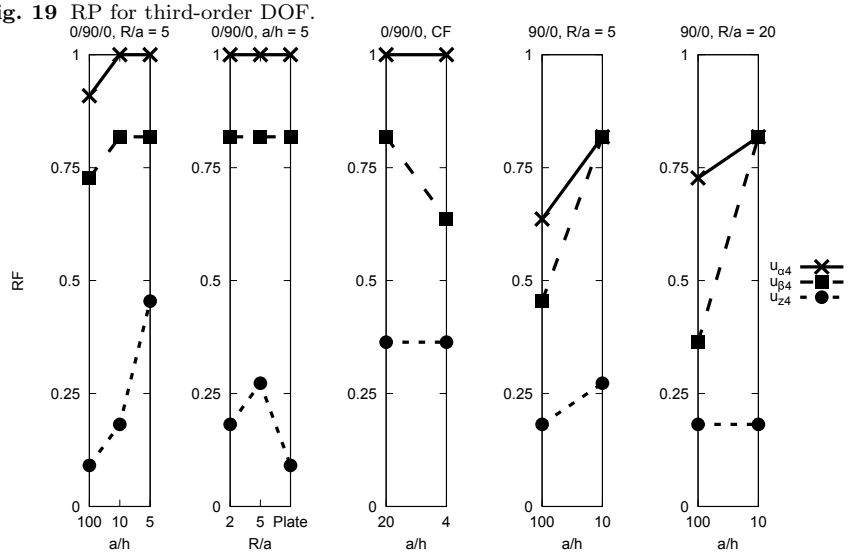

Fig. 20 RP for fourth-order DOF.

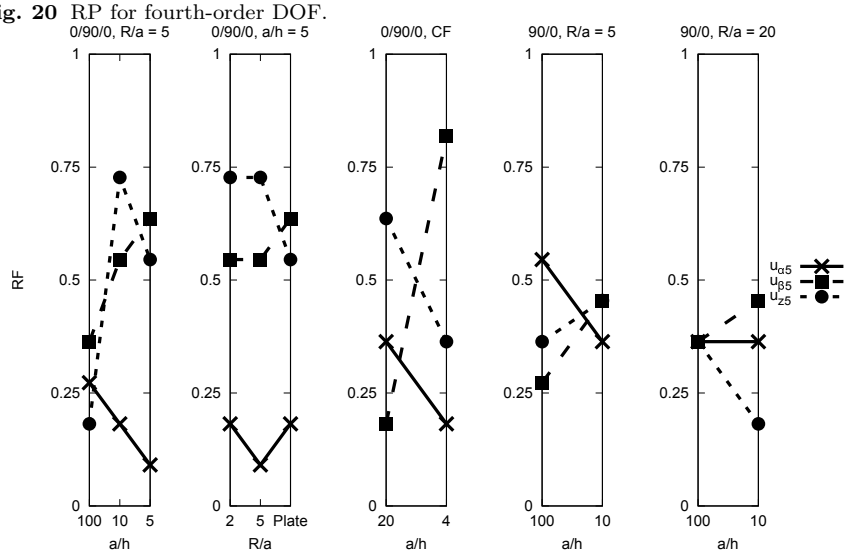

Fig. 21 BTD for 0/90/0, R/a = 5, with seven and nine DOF models

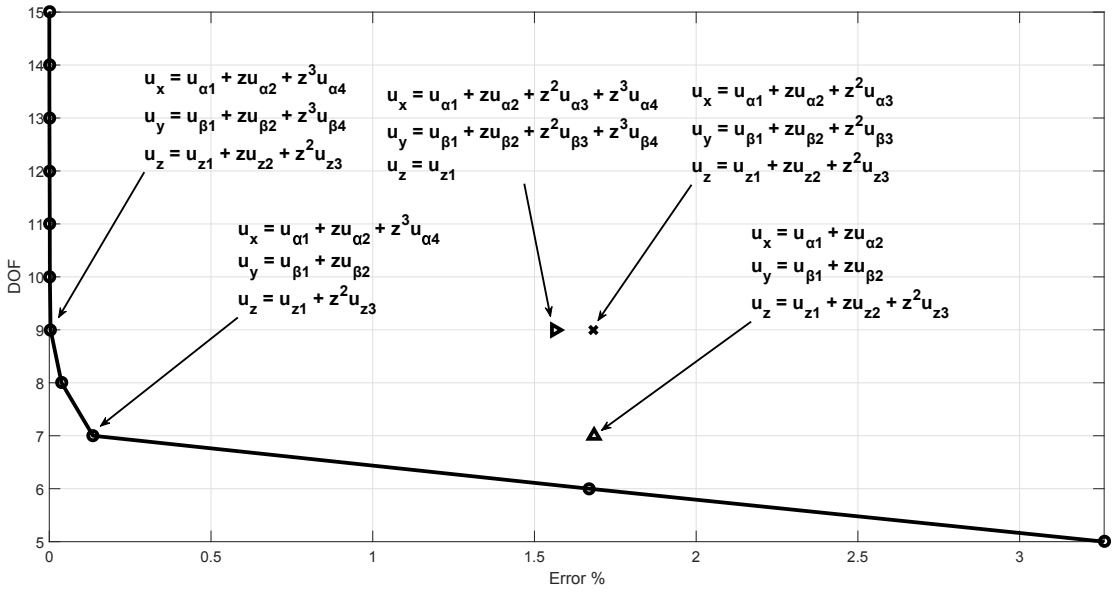

(a) a/h = 100

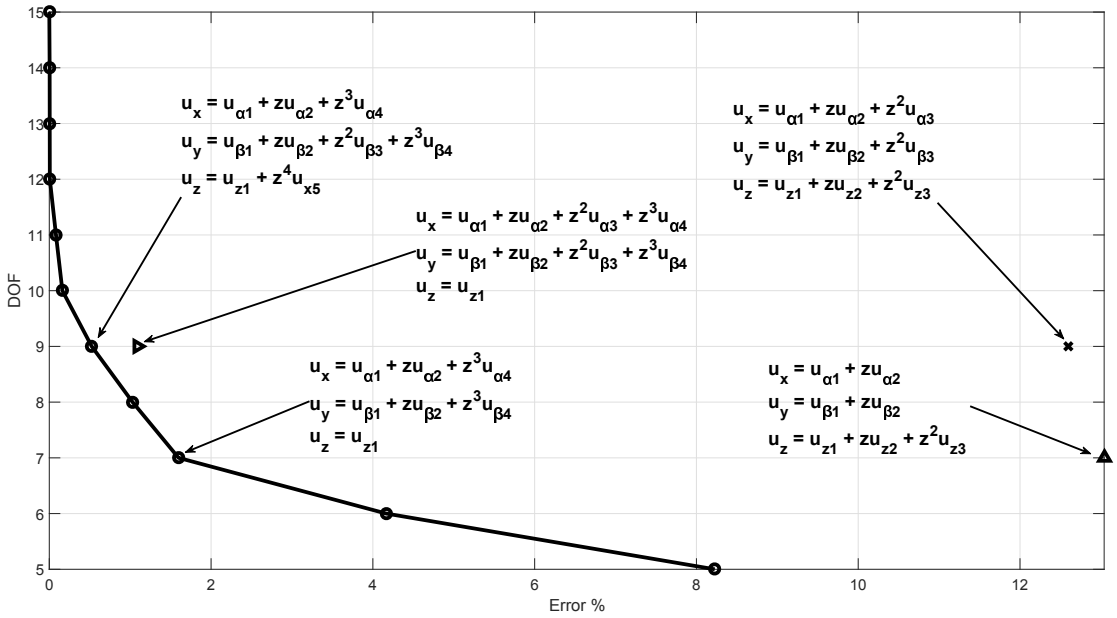

(b) a/h = 10

Fig. 22 BTD for 90/0, R/a = 5, with seven and nine DOF models

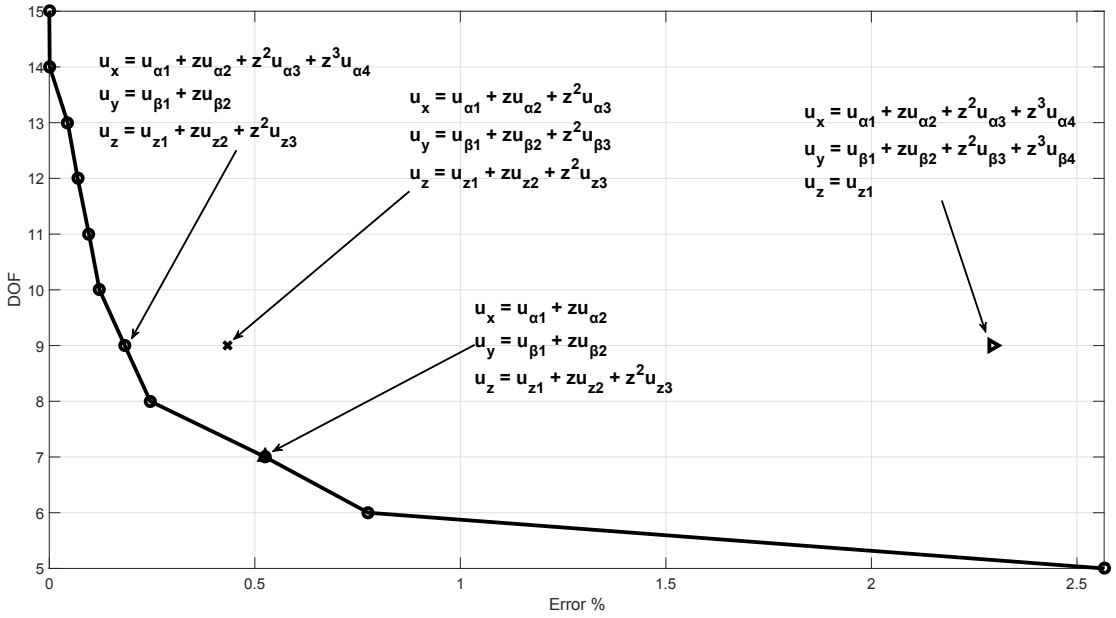

(a) a/h = 100

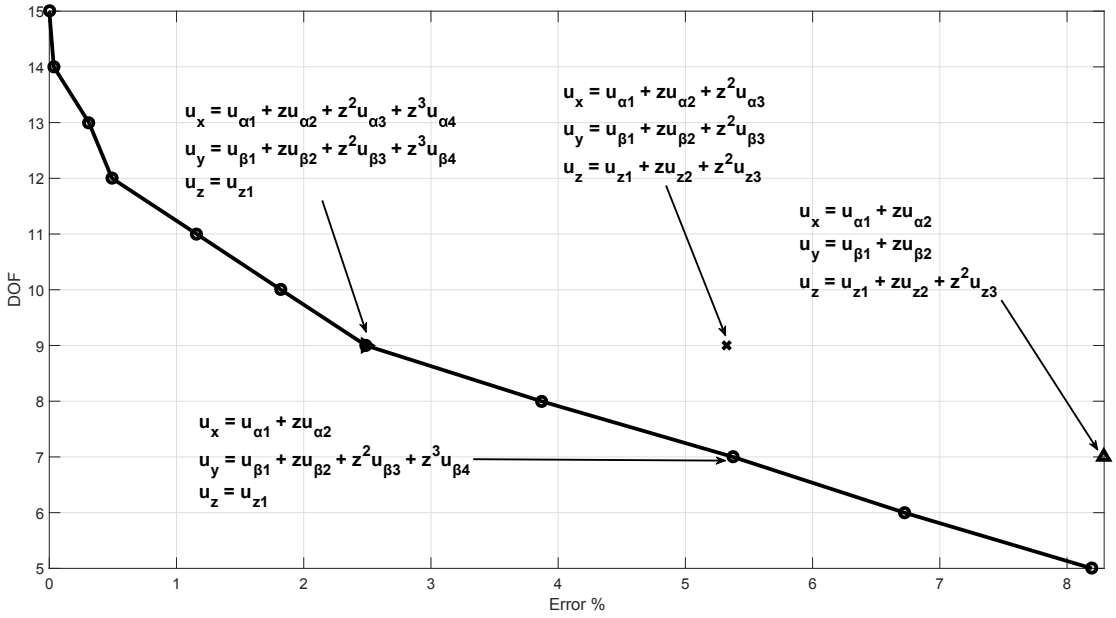

(b) a/h = 10

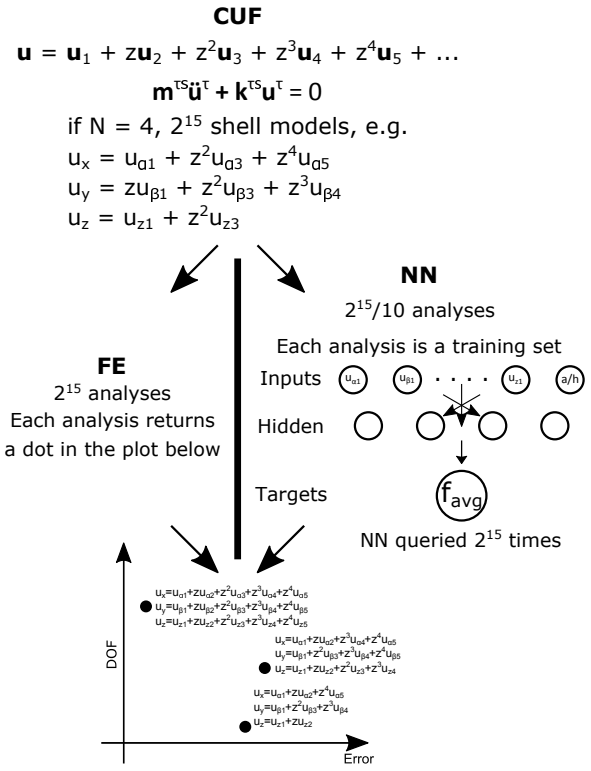

Fig. 23 CUF and NN.

Tables

Table 1 Shell finite elements assessed

	DOF	u_{α_1}	u_{β_1}	u_{z1}	u_{α_2}	u_{β_2}	u_{z2}	u_{α_3}	u_{β_3}	u_{z3}	u_{α_4}	u_{β_4}	u_{z4}	u_{α_5}	u_{β_5}	u_{z5}
N=4	15	▲	▲	▲	▲	▲	▲	▲	▲	▲	▲	▲	▲	▲	▲	▲
N=3	12	▲	▲	▲	▲	▲	▲	▲	▲	▲	▲	▲	▲	△	△	△
TSDT	9	▲	▲	▲	▲	▲	△	▲	▲	△	▲	▲	△	△	△	△
N=2	9	▲	▲	▲	▲	▲	▲	▲	▲	▲	△	△	△	△	△	△
PTD	7	▲	▲	▲	▲	▲	▲	△	△	▲	△	△	△	△	△	△
FSDT	5	▲	▲	▲	▲	▲	△	△	△	△	△	△	△	△	△	△

Table 2 0/90/0, a/h = 10, $\overline{\omega} = \omega\sqrt{\frac{\rho a^4}{h^2 E_T}}$.

Model	R/a = 2	R/a = 5	Plate
HSDT [28]	-	12.060	11.790
FSDT [26]	13.382	12.372	12.162
CLT [184]	15.878	15.233	15.104
LD4 [201]	12.773	11.685	11.457
N=4	13.007	11.972	11.756

Table 3 BTD models for 0/90/0, R/a = 5, a/h = 100

DOF	u_{α_1}	u_{β_1}	u_{z1}	u_{α_2}	u_{β_2}	u_{z2}	u_{α_3}	u_{β_3}	u_{z3}	u_{α_4}	u_{β_4}	u_{z4}	u_{α_5}	u_{β_5}	u_{z5}
15	▲	▲	▲	▲	▲	▲	▲	▲	▲	▲	▲	▲	▲	▲	▲
14	▲	▲	▲	▲	▲	▲	▲	▲	▲	▲	▲	△	▲	▲	▲
13	▲	▲	▲	▲	▲	▲	▲	▲	▲	▲	▲	△	▲	▲	△
12	▲	▲	▲	▲	▲	▲	▲	▲	▲	▲	▲	△	△	▲	△
11	▲	▲	▲	▲	▲	▲	▲	▲	▲	▲	▲	△	△	△	△
10	▲	▲	▲	▲	▲	▲	△	▲	▲	▲	▲	△	△	△	△
9	▲	▲	▲	▲	▲	▲	△	△	▲	▲	▲	△	△	△	△
8	▲	▲	▲	▲	▲	△	△	△	▲	▲	▲	△	△	△	△
7	▲	▲	▲	▲	▲	△	△	△	▲	▲	△	△	△	△	△
6	▲	▲	▲	▲	▲	△	△	△	△	▲	△	△	△	△	△
5	▲	▲	▲	▲	▲	△	△	△	△	△	△	△	△	△	△
	$RF_0 = 1.00$			$RF_1 = 0.88$			$RF_2 = 0.61$			$RF_3 = 0.58$			$RF_4 = 0.27$		

Table 4 BTD models for 0/90/0, R/a = 5, a/h = 10

DOF	u_{α_1}	u_{β_1}	u_{z1}	u_{α_2}	u_{β_2}	u_{z2}	u_{α_3}	u_{β_3}	u_{z3}	u_{α_4}	u_{β_4}	u_{z4}	u_{α_5}	u_{β_5}	u_{z5}
15	▲	▲	▲	▲	▲	▲	▲	▲	▲	▲	▲	▲	▲	▲	▲
14	▲	▲	▲	▲	▲	▲	△	▲	▲	▲	▲	▲	▲	▲	▲
13	▲	▲	▲	▲	▲	▲	▲	▲	▲	▲	▲	△	△	▲	▲
12	▲	▲	▲	▲	▲	▲	△	▲	▲	▲	▲	△	△	▲	▲
11	▲	▲	▲	▲	▲	▲	△	▲	△	▲	▲	△	△	▲	▲
10	▲	▲	▲	▲	▲	△	△	▲	△	▲	▲	△	△	▲	▲
9	▲	▲	▲	▲	▲	△	△	▲	△	▲	▲	△	△	△	▲
8	▲	▲	▲	▲	▲	△	△	△	△	▲	▲	△	△	△	▲
7	▲	▲	▲	▲	▲	△	△	△	△	▲	▲	△	△	△	△
6	▲	▲	▲	▲	▲	△	△	△	△	▲	△	△	△	△	△
5	▲	▲	▲	△	▲	△	△	△	△	▲	△	△	△	△	△
	$RF_0 = 1.00$			$RF_1 = 0.79$			$RF_2 = 0.39$			$RF_3 = 0.67$			$RF_4 = 0.48$		

Table 5 BTD models for 0/90/0, R/a = 5, a/h = 5

DOF	u_{α_1}	u_{β_1}	u_{z1}	u_{α_2}	u_{β_2}	u_{z2}	u_{α_3}	u_{β_3}	u_{z3}	u_{α_4}	u_{β_4}	u_{z4}	u_{α_5}	u_{β_5}	u_{z5}
15	▲	▲	▲	▲	▲	▲	▲	▲	▲	▲	▲	▲	▲	▲	▲
14	▲	▲	▲	▲	▲	▲	▲	▲	▲	▲	▲	▲	△	▲	▲
13	▲	▲	▲	▲	▲	▲	△	▲	▲	▲	▲	▲	△	▲	▲
12	▲	▲	▲	▲	▲	△	△	▲	▲	▲	▲	▲	△	▲	▲
11	▲	▲	▲	▲	▲	△	△	▲	△	▲	▲	▲	△	▲	▲
10	▲	▲	▲	▲	▲	△	△	▲	△	▲	▲	△	△	▲	▲
9	▲	▲	▲	▲	▲	△	△	▲	△	▲	▲	△	△	▲	△
8	▲	▲	▲	▲	▲	△	△	▲	△	▲	▲	△	△	△	△
7	▲	▲	▲	▲	▲	△	△	△	△	▲	▲	△	△	△	△
6	▲	▲	▲	▲	▲	△	△	△	△	▲	△	△	△	△	△
5	▲	▲	▲	△	▲	△	△	△	△	▲	△	△	△	△	△
	$RF_0 = 1.00$			$RF_1 = 0.73$			$RF_2 = 0.42$			$RF_3 = 0.76$			$RF_4 = 0.39$		

Table 6 BTD models for 0/90/0, R/a = 2, a/h = 10

DOF	u_{α_1}	u_{β_1}	u_{z1}	u_{α_2}	u_{β_2}	u_{z2}	u_{α_3}	u_{β_3}	u_{z3}	u_{α_4}	u_{β_4}	u_{z4}	u_{α_5}	u_{β_5}	u_{z5}
15	▲	▲	▲	▲	▲	▲	▲	▲	▲	▲	▲	▲	▲	▲	▲
14	▲	▲	▲	▲	▲	▲	▲	▲	▲	▲	▲	▲	△	▲	▲
13	▲	▲	▲	▲	▲	▲	△	▲	▲	▲	▲	▲	△	▲	▲
12	▲	▲	▲	▲	▲	▲	△	▲	▲	▲	▲	△	△	▲	▲
11	▲	▲	▲	▲	▲	△	△	▲	▲	▲	▲	△	△	▲	▲
10	▲	▲	▲	▲	▲	△	△	▲	△	▲	▲	△	△	▲	▲
9	▲	▲	▲	▲	▲	△	△	▲	△	▲	▲	△	△	△	▲
8	▲	▲	▲	▲	▲	△	△	△	△	▲	▲	△	△	△	▲
7	▲	▲	▲	▲	▲	△	△	△	△	▲	▲	△	△	△	△
6	▲	▲	▲	▲	▲	△	△	△	△	▲	△	△	△	△	△
5	▲	▲	▲	△	▲	△	△	△	△	▲	△	△	△	△	△
	$RF_0 = 1.00$			$RF_1 = 0.76$			$RF_2 = 0.42$			$RF_3 = 0.70$			$RF_4 = 0.45$		

Table 7 BTD models for 0/90/0, Plate, a/h = 10

DOF	u_{α_1}	u_{β_1}	u_{z1}	u_{α_2}	u_{β_2}	u_{z2}	u_{α_3}	u_{β_3}	u_{z3}	u_{α_4}	u_{β_4}	u_{z4}	u_{α_5}	u_{β_5}	u_{z5}
15	▲	▲	▲	▲	▲	▲	▲	▲	▲	▲	▲	▲	▲	▲	▲
14	▲	▲	▲	▲	▲	▲	▲	▲	▲	▲	▲	△	▲	▲	▲
13	▲	▲	▲	▲	▲	▲	▲	▲	▲	▲	▲	△	△	▲	▲
12	▲	▲	▲	▲	▲	▲	△	▲	▲	▲	▲	△	△	▲	▲
11	▲	▲	▲	▲	▲	△	△	▲	▲	▲	▲	△	△	▲	▲
10	▲	▲	▲	▲	▲	△	△	▲	▲	▲	▲	△	△	▲	△
9	▲	▲	▲	▲	▲	△	△	▲	△	▲	▲	△	△	▲	△
8	▲	▲	▲	▲	▲	△	△	△	△	▲	▲	△	△	△	▲
7	▲	▲	▲	▲	▲	△	△	△	△	▲	▲	△	△	△	△
6	▲	▲	▲	▲	▲	△	△	△	△	▲	△	△	△	△	△
5	▲	▲	▲	△	▲	△	△	△	△	▲	△	△	△	△	△
	$RF_0 = 1.00$			$RF_1 = 0.73$			$RF_2 = 0.49$			$RF_3 = 0.64$			$RF_4 = 0.45$		

Table 8 0/90/0, clamped-free, R/a = 10, $\overline{\omega} = \omega\sqrt{\frac{\rho a^4}{h^2 E_T}}$.

Model	a/h = 4	a/h = 20
LD4 [201]	7.094	23.505
N=4	7.250	24.144

Table 9 BTD models for 0/90/0, clamped-free, R/a = 10, a/h = 20

DOF	u_{α_1}	u_{β_1}	u_{z1}	u_{α_2}	u_{β_2}	u_{z2}	u_{α_3}	u_{β_3}	u_{z3}	u_{α_4}	u_{β_4}	u_{z4}	u_{α_5}	u_{β_5}	u_{z5}
15	▲	▲	▲	▲	▲	▲	▲	▲	▲	▲	▲	▲	▲	▲	▲
14	▲	▲	▲	▲	▲	▲	▲	▲	▲	▲	▲	▲	▲	△	▲
13	▲	▲	▲	▲	▲	▲	△	▲	▲	▲	▲	▲	▲	△	▲
12	▲	▲	▲	▲	▲	▲	△	△	▲	▲	▲	▲	▲	△	▲
11	▲	▲	▲	▲	▲	△	△	▲	▲	▲	▲	△	△	▲	▲
10	▲	▲	▲	▲	▲	△	△	▲	▲	▲	▲	△	△	△	▲
9	▲	▲	▲	▲	▲	△	△	△	▲	▲	▲	△	△	△	▲
8	▲	▲	▲	▲	▲	△	△	△	▲	▲	▲	△	△	△	△
7	▲	▲	▲	▲	▲	△	△	△	△	▲	▲	△	△	△	△
6	▲	▲	▲	▲	▲	△	△	△	△	▲	△	△	△	△	△
5	▲	▲	▲	△	▲	△	△	△	△	▲	△	△	△	△	△
	$RF_0 = 1.00$			$RF_1 = 0.76$			$RF_2 = 0.45$			$RF_3 = 0.73$			$RF_4 = 0.40$		

Table 10 BTD models for 0/90/0, clamped-free, R/a = 10, a/h = 4

DOF	u_{α_1}	u_{β_1}	u_{z1}	u_{α_2}	u_{β_2}	u_{z2}	u_{α_3}	u_{β_3}	u_{z3}	u_{α_4}	u_{β_4}	u_{z4}	u_{α_5}	u_{β_5}	u_{z5}
15	▲	▲	▲	▲	▲	▲	▲	▲	▲	▲	▲	▲	▲	▲	▲
14	▲	▲	▲	▲	▲	▲	△	▲	▲	▲	▲	▲	▲	▲	▲
13	▲	▲	▲	▲	▲	▲	△	▲	▲	▲	▲	▲	△	▲	▲
12	▲	▲	▲	▲	▲	▲	△	▲	▲	▲	▲	▲	△	▲	△
11	▲	▲	▲	▲	▲	▲	△	▲	△	▲	▲	△	△	▲	▲
10	▲	▲	▲	▲	▲	▲	△	▲	△	▲	▲	△	△	▲	△
9	▲	▲	▲	▲	▲	△	△	▲	△	▲	▲	△	△	▲	△
8	▲	▲	▲	▲	▲	△	△	▲	△	▲	△	△	△	▲	△
7	▲	▲	▲	△	▲	△	△	▲	△	▲	△	△	△	▲	△
6	▲	▲	▲	△	▲	△	△	▲	△	▲	△	△	△	△	△
5	▲	▲	▲	△	▲	△	△	△	△	▲	△	△	△	△	△
	$RF_0 = 1.00$			$RF_1 = 0.76$			$RF_2 = 0.45$			$RF_3 = 0.67$			$RF_4 = 0.45$		

Table 11 90/0, $\overline{\omega} = \omega\sqrt{\frac{\rho a^4}{h^2 E_T}}$.

Model	R/a = 5	R/a = 20
	a/h = 100	
HSDT [28]	28.840	11.84
N=4	28.824	11.842
	a/h = 10	
HSDT [28]	9.377	8.999
N=4	9.269	8.967

Table 12 BTD models for 90/0, R/a = 5, a/h = 100

DOF	u_{α_1}	u_{β_1}	u_{z1}	u_{α_2}	u_{β_2}	u_{z2}	u_{α_3}	u_{β_3}	u_{z3}	u_{α_4}	u_{β_4}	u_{z4}	u_{α_5}	u_{β_5}	u_{z5}
15	▲	▲	▲	▲	▲	▲	▲	▲	▲	▲	▲	▲	▲	▲	▲
14	▲	▲	▲	▲	▲	▲	▲	▲	▲	▲	▲	△	▲	▲	▲
13	▲	▲	▲	▲	▲	▲	▲	▲	▲	▲	▲	△	▲	△	▲
12	▲	▲	▲	▲	▲	▲	▲	▲	▲	▲	▲	△	▲	△	△
11	▲	▲	▲	▲	▲	▲	▲	△	▲	▲	△	△	▲	▲	△
10	▲	▲	▲	▲	▲	▲	△	▲	▲	▲	▲	△	△	△	△
9	▲	▲	▲	▲	▲	▲	▲	△	▲	△	△	△	▲	△	△
8	▲	▲	▲	▲	▲	▲	△	△	▲	▲	△	△	△	△	△
7	▲	▲	▲	▲	▲	△	△	△	▲	△	△	▲	△	△	△
6	▲	▲	▲	▲	▲	△	△	△	△	△	△	△	△	△	▲
5	▲	▲	▲	▲	▲	△	△	△	△	△	△	△	△	△	△
	$RF_0 = 1.00$			$RF_1 = 0.91$			$RF_2 = 0.61$			$RF_3 = 0.42$			$RF_4 = 0.39$		

Table 13 BTD models for 90/0, R/a = 5, a/h = 10

DOF	u_{α_1}	u_{β_1}	u_{z1}	u_{α_2}	u_{β_2}	u_{z2}	u_{α_3}	u_{β_3}	u_{z3}	u_{α_4}	u_{β_4}	u_{z4}	u_{α_5}	u_{β_5}	u_{z5}
15	▲	▲	▲	▲	▲	▲	▲	▲	▲	▲	▲	▲	▲	▲	▲
14	▲	▲	▲	▲	▲	▲	▲	▲	▲	▲	▲	▲	▲	▲	△
13	▲	▲	▲	▲	▲	△	▲	▲	△	▲	▲	▲	▲	▲	▲
12	▲	▲	▲	▲	▲	△	▲	▲	△	▲	▲	△	▲	▲	▲
11	▲	▲	▲	▲	▲	△	▲	▲	△	▲	▲	△	△	▲	▲
10	▲	▲	▲	▲	▲	△	▲	▲	△	▲	▲	△	△	△	▲
9	▲	▲	▲	▲	▲	△	▲	▲	△	▲	▲	△	△	△	△
8	▲	▲	▲	▲	▲	△	△	▲	△	▲	▲	△	△	△	△
7	▲	▲	▲	▲	▲	△	△	△	△	▲	▲	△	△	△	△
6	▲	▲	▲	▲	▲	△	△	△	△	▲	△	△	△	△	△
5	▲	▲	▲	▲	▲	△	△	△	△	△	△	△	△	△	△
	$RF_0 = 1.00$			$RF_1 = 0.73$			$RF_2 = 0.52$			$RF_3 = 0.67$			$RF_4 = 0.42$		

Table 14 BTD models for 90/0, R/a = 20, a/h = 100

DOF	u_{α_1}	u_{β_1}	u_{z1}	u_{α_2}	u_{β_2}	u_{z2}	u_{α_3}	u_{β_3}	u_{z3}	u_{α_4}	u_{β_4}	u_{z4}	u_{α_5}	u_{β_5}	u_{z5}
15	▲	▲	▲	▲	▲	▲	▲	▲	▲	▲	▲	▲	▲	▲	▲
14	▲	▲	▲	▲	▲	▲	▲	▲	▲	▲	▲	△	▲	▲	▲
13	▲	▲	▲	▲	▲	▲	▲	▲	▲	▲	△	▲	▲	▲	△
12	▲	▲	▲	▲	▲	▲	▲	△	▲	▲	▲	△	▲	△	▲
11	▲	▲	▲	▲	▲	▲	▲	▲	▲	▲	△	△	△	▲	△
10	▲	▲	▲	▲	▲	▲	▲	△	▲	▲	▲	△	△	△	△
9	▲	▲	▲	▲	▲	▲	▲	△	▲	▲	△	△	△	△	△
8	▲	▲	▲	▲	▲	▲	△	△	▲	▲	△	△	△	△	△
7	▲	▲	▲	▲	▲	▲	△	△	▲	△	△	△	△	△	△
6	▲	▲	▲	▲	▲	△	△	△	▲	△	△	△	△	△	△
5	▲	▲	▲	▲	▲	△	△	△	△	△	△	△	△	△	△
	$RF_0 = 1.00$			$RF_1 = 0.94$			$RF_2 = 0.64$			$RF_3 = 0.42$			$RF_4 = 0.33$		

Table 15 BTD models for 90/0, R/a = 20, a/h = 10

DOF	u_{α_1}	u_{β_1}	u_{z1}	u_{α_2}	u_{β_2}	u_{z2}	u_{α_3}	u_{β_3}	u_{z3}	u_{α_4}	u_{β_4}	u_{z4}	u_{α_5}	u_{β_5}	u_{z5}
15	▲	▲	▲	▲	▲	▲	▲	▲	▲	▲	▲	▲	▲	▲	▲
14	▲	▲	▲	▲	▲	▲	▲	▲	▲	▲	▲	▲	▲	▲	△
13	▲	▲	▲	▲	▲	▲	▲	▲	▲	▲	▲	△	▲	▲	△
12	▲	▲	▲	▲	▲	△	▲	▲	▲	▲	▲	△	▲	▲	△
11	▲	▲	▲	▲	▲	△	▲	▲	▲	▲	▲	△	△	▲	△
10	▲	▲	▲	▲	▲	△	▲	▲	△	▲	▲	△	△	△	▲
9	▲	▲	▲	▲	▲	△	▲	▲	△	▲	▲	△	△	△	△
8	▲	▲	▲	▲	▲	△	△	▲	△	▲	▲	△	△	△	△
7	▲	▲	▲	▲	▲	△	△	▲	△	△	▲	△	△	△	△
6	▲	▲	▲	▲	▲	△	△	△	△	▲	△	△	△	△	△
5	▲	▲	▲	▲	▲	△	△	△	△	△	△	△	△	△	△
	$RF_0 = 1.00$			$RF_1 = 0.76$			$RF_2 = 0.64$			$RF_3 = 0.61$			$RF_4 = 0.33$		

Table 16 Overview of FE and NN computational costs to obtain BTD.

Process	Analyses	Cost
BTD via FE	2^{15} eigenvalue problems	1
Data training generation	$2^{15}/10$ eigenvalue problems	0.1
Training of NN	One layer with ten neurons	0.02
BTD via NN	2^{15} queries to NN	0.001